Energy &
Environmental Science

RSCPublishing

REVIEW

View Article Online
View Journal | View Issue

Cite this: *Energy Environ. Sci.*, 2013, **6**, 2338

Room-temperature stationary sodium-ion batteries for large-scale electric energy storage†

Huilin Pan, Yong-Sheng Hu* and Liquan Chen

Received 11th March 2013
Accepted 26th June 2013

DOI: 10.1039/c3ee40847g

www.rsc.org/ees

Room-temperature stationary sodium-ion batteries have attracted great attention particularly in large-scale electric energy storage applications for renewable energy and smart grid because of the huge abundant sodium resources and low cost. In this article, a variety of electrode materials including cathodes and anodes as well as electrolytes for room-temperature stationary sodium-ion batteries are briefly reviewed. We compare the difference in storage behavior between Na and Li in their analogous electrodes and summarize the sodium storage mechanisms in the available electrode materials. This review also includes some new results from our group and our thoughts on developing new materials. Some perspectives and directions on designing better materials for practical applications are pointed out based on knowledge from the literature and our experience. Through this extensive literature review, the search for suitable electrode and electrolyte materials for stationary sodium-ion batteries is still challenging. However, after intensive research efforts, we believe that low-cost, long-life and room-temperature sodium-ion batteries would be promising for applications in large-scale energy storage system in the near future.

Broader context

With the rapid development of renewable energy sources, such as the wind and the sun, large-scale electric energy storage systems are becoming extremely important to realize the smooth integration of these intermittent energies into the grid. Among the potential energy storage technologies, electrochemical secondary battery technology is one of the most promising means of storing electricity on a large-scale because of flexibility, high energy conversion efficiency and simple maintenance. So far, lithium-ion batteries are the most successfully developed technology, have been widely used in portable electronic devices and have been regarded as the best choice for (hybrid) electric vehicles. The latter application raises concern for a possible shortage of the limited lithium resources in the Earth's crust. Therefore, alternatively, room-temperature sodium-ion batteries have again aroused a great deal of interest recently, particularly for large-scale stationary energy storage applications, due to the practically infinite sodium resources and their low cost. This review is intended to provide a wider literature overview and present our perspective on designing better materials for stationary sodium-ion batteries to realize practical applications in the near future.

1 Introduction

Energy production, a material base that supports our society, is becoming more and more important. With the imminent exhaustion of fossil fuel resources and increasing environmental problems, a variety of renewable and clean energy sources, such as the wind and sun, are growing rapidly. However, the increasing use of renewable energy sources also brings other problems, such as modulating variable renewable resources from time to time and integrating them into the grid smoothly and safely. Balancing electricity generation and demand between daytime and nighttime is also important to optimize grid utilization. Thus a large-scale energy storage system (ESS) is extremely important to shift electrical energy from peak to off-peak periods to realize smart grid management. A number of potential technologies have been proposed for renewable energy and utility applications, such as pump hydro, compressed air, fly-wheel and electrochemical batteries.[1–4] Among various energy storage technologies, the secondary battery technique is one of the most promising means for storing electricity on a large-scale because of flexibility, high energy conversion efficiency and simple maintenance.[1] The major parameters of stationary batteries for ESS are significantly different from those of power batteries used in electric vehicles (EV). Long cycle life, low cost, and high safety are the most important parameters. Hence, an abundant, non-toxic, stable and low-strain electrode material needs to be developed to ensure large-scale and long-term applications, and to decrease battery management cost.

Key Laboratory for Renewable Energy, Beijing Key Laboratory for New Energy Materials and Devices, Beijing National Laboratory for Condensed Matter Physics, Institute of Physics, Chinese Academy of Sciences, Beijing 100190, China. E-mail: yshu@aphy.iphy.ac.cn

† Electronic supplementary information (ESI) available. See DOI: 10.1039/c3ee40847g

To date, sodium–sulfur (Na–S) batteries, flow batteries and lithium-ion (Li-ion) batteries have been considered as potential energy storage devices for ESS.[1–6] Particularly, practical applications of Li-ion batteries with the highest energy density and long cycle life have been realized and have attracted extensive attention.[1] However, the large-scale demand for Li would force us to consider the growing price of Li resources because of the low abundance of Li in the Earth's crust as shown in Fig. 1.[7] Based on calculations, total global Li consumption in 2008 was approximately 21 280 tons; hence mineable Li resources from the present could be sustained for approximately 65 years at most, considering an average growth of 5% per year.[8] Note that the EV market consumption of Li was not considered fully. Therefore, there is an urgent and desired need to explore low-cost, highly safe, and cycling stable rechargeable batteries based on abundant resources. Compared with Li, Na has similar physical and chemical properties. However, Na is very abundant and low cost, as shown in Table 1.[9–12] Note that the gravimetric and volumetric densities of Na-ion battery would not exceed those of its Li analogue because of the relatively heavier and larger Na atom and less-reducing potential of Na. However, energy density is not a critical issue in the field of large-scale ESS. Thus, developing room-temperature "rocking-chair" Na-ion batteries with a similar working principle as Li-ion batteries (Fig. 2) for large-scale ESS is still a reasonable alternative.

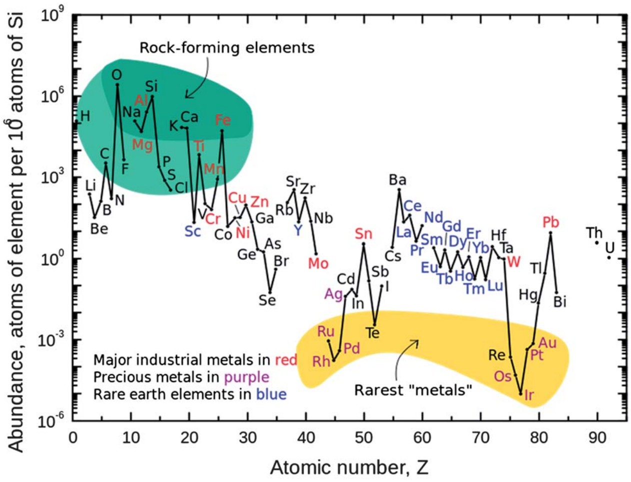

Fig. 1 The abundance of chemical elements in Earth's crust[7] (Wikipedia).

Na-based batteries are not new. From the 1970s to the 1980s, Na-ion and Li-ion batteries were investigated in parallel.[13–18] The investigation of Na-ion batteries was significantly decreased after the success of the commercial application of Li-ion batteries in the 1990s. Moreover, Na–S battery has already been commercially demonstrated.[10,19] Nevertheless, the safety issue of molten Na and sulphur at 300–350 °C in Na–S batteries is still a tough problem for large-scale applications. Recently, research interest in Na-ion batteries operated at room-temperature is renewed because of the abundance and low cost of Na. Previously, the Na intercalation into layered MoS_2, TaS_2, TiS_2 and Na_xMO_2 (M=Co, Mn, *etc.*) was primarily investigated by Whittingham and Hagenmuller during the 1970s to the 1980s.[15–18] However, searching for new electrode materials (cathode and anode) and new stable electrolytes (liquid and solid) for Na-ion battery system is necessary. The present high throughput *ab initio* calculation first proposed by Ceder's group could provide a possible shortcut to immediately identify new useful electrode

---

Huilin Pan received her MSc degree (2010) and PhD degree (2013) in condensed matter physics from Jilin University and the Institute of Physics, Chinese Academy of Sciences, respectively. Her recent research interests include developing new materials for low-cost energy storage devices, the energy storage mechanism and advanced electrode material characterizations.

Yong-Sheng Hu is a professor at the Institute of Physics, Chinese Academy of Sciences (IOP-CAS). He received his PhD at IOP-CAS with Prof. Liquan Chen in 2004, and then moved to Max Planck Institute for Solid State Research as a postdoctoral fellow in Prof. Joachim Maier's Department. After a short stay at Prof. Eric McFarland's group in the University of California at Santa Barbara, he joined IOP-CAS in 2008 and is currently working on advanced materials for high-energy density batteries (e.g., Li–S batteries) and long-life grid-scale stationary batteries (e.g., sodium-ion batteries).

Liquan Chen is a professor at the Institute of Physics, Chinese Academy of Sciences (IOP-CAS). He has being working in the field of solid state ionics for a long time. His research activities are related to ion and/or electron transport in materials. He is especially interested in new materials and new systems for energy storage.

Table 1 The comparison between Na and Li elements[9–12]

	Na	Li
Cation radius	97 pm	68 pm
Atomic weight	23 g mol^{-1}	6.9 g mol^{-1}
E_o *vs.* SHE	−2.7 V	−3.04 V
A–O coordination	Octahedral or prismatic	Octahedral or tetrahedral
Melting point	97.7 °C	180.5 °C
Abundance	23.6×10^3 mg kg^{-1}	20 mg kg^{-1}
Distribution	Everywhere	70% in South America
Price, carbonates	~2 RMB per kg	~40 RMB per kg

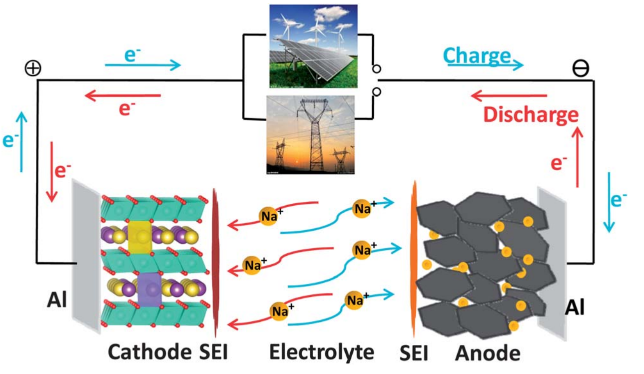

Fig. 2 The working principle of room-temperature "rocking chair" sodium-ion batteries.

materials.[20,21] Furthermore, fundamental scientific questions need to be further elucidated, including (1) the difference in transport and kinetic behaviors between Na and Li in analogous electrodes; (2) Na insertion/extraction mechanism; (3) solid electrolyte interphase (SEI) layer on the electrodes from different electrolyte systems; and (4) charge transfer in the electrolyte–electrode interface and Na^+ ion transport through the SEI layer.

Aside from the organic liquid electrolyte based system, developing aqueous Na-ion batteries rather than Li-ion batteries is another important aspect in further enhancing the safety issue and decreasing the cost.[22–29] Expensive organic liquid electrolytes can be replaced by aqueous electrolytes, and cheap inorganic Na salts, such as Na_2SO_4 and $NaNO_3$, can be used in a large-scale.[28,29]

In this review, we focus on (1) currently available cathode and anode materials, including both inorganic and organic ones; (2) organic liquid and solid electrolytes for Na-ion batteries; (3) Na storage mechanism *vs.* Li storage; (4) present high throughput *ab initio* calculations and (5) the aqueous Na-ion battery system. Most Na electrode materials available at present are derived from their Li analogues. Even the electrode materials for Li-ion batteries are also tested for Na storage, which is probably a means for exploring the right electrode for Na-ion batteries. However, numerous invalid trials waste resources and confuse the path towards the right direction for Na-ion batteries. We are attempting to introduce several directions to develop room-temperature Na-ion battery *via* a review of existing research on Na-ion batteries.

2 Cathode materials

2.1 Layered transition metal (TM) oxides

The structure and physical properties of lamellar A_xMO_{2+y} (A = alkali, M = Transition metal) were extensively investigated during the 1970s and 1980s.[16,17] The layered structure is built by sheets of edge-shared MO_6 octahedra, wherein alkali ions are located between MO_6 sheets. Delmas and co-workers first specified A_xMO_2 compounds by describing the stacking arrangements of alkali ions between layers.[16] O or P represents octahedral or trigonal prismatic coordination environment of alkali ions (note that as far as we know, Li cannot occupy the trigonal prismatic site in the case of Li containing layered compounds because of the smaller ionic size of Li.); the number 3 or 2 describes the number of TM layers in a repeated stacking unit, and O′3 and P′2 represent the monoclinic distortion of O3 and P2 phase packing. The stacking types of O3 and P2 phases are shown in Fig. 3. Delmas and co-workers originally performed pioneering work on reversible structural transition in alkali ion insertion/extraction processes.[30] The phase transition O3 → O′3 → P′3 often occurs, whereas P2 phase is different from P3 and O3. A phase transition from the P2 phase requires a π/3 rotation of MO_6 octahedral and a breaking of M–O bonds, thus the P2 phase generally retains its structure during the electrochemical reactions. So far, layered $LiCoO_2$ is the most successful cathode material with high energy density used in Li-ion batteries since its commercial application in 1990s by Sony. The Na analogue of this type of battery exhibits an electrochemical intercalation behavior similar to $LiMO_2$ but with more complex phase transitions during the removal of Na^+ ions from alkali ion layers. This behavior is also common for other Na compounds (*e.g.*, $Na_{0.44}MnO_2$),[31,32] which might be due to larger Na^+ ions, longer A–O bonds and the ordering arrangement between Na^+ and V_{Na+} (forming the ordered structure) and/or charge ordering at different Na contents.

In the 1980s, $NaCoO_2$ was an early choice of a Na transition metal oxide to be tested for its Na intercalation behaviors in the

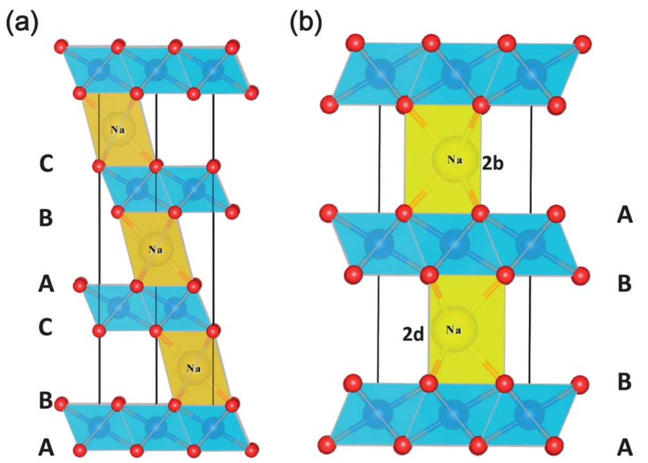

Fig. 3 The stacking types of (a) O3 and (b) P2 phases in A_xMO_{2+y}. In particular, in the P2-structure, there are two different sites for Na ions. One occupies the 2d site sharing the edges with the MO_6 octahedra whereas the other occupies the 2b site sharing two faces with the MO_6 octahedra.

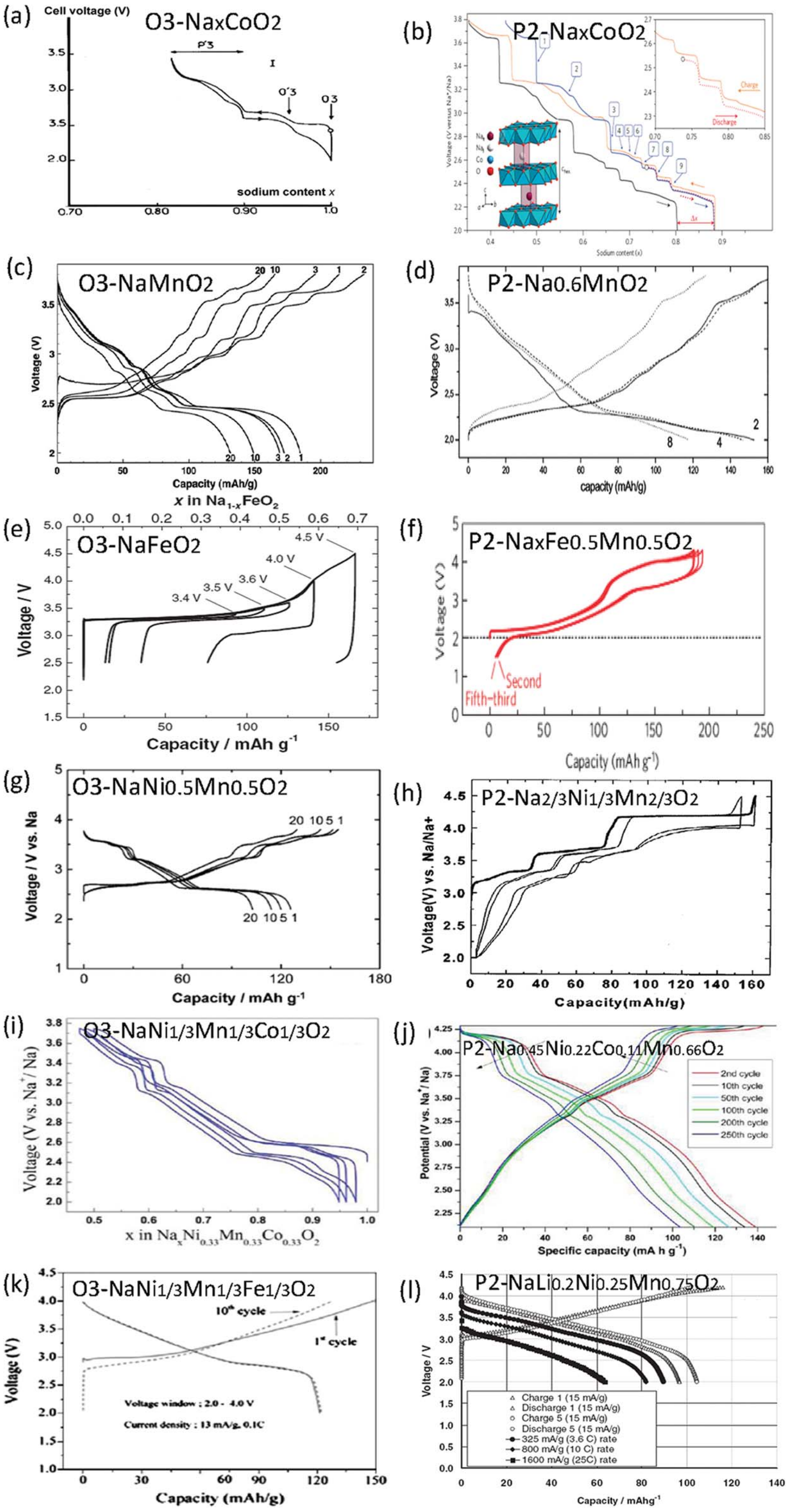

Fig. 4 The charge–discharge profiles of (a) $NaCoO_2$ (Reproduced with permission.[30] Copyright 1981, Elsevier.), (b) P2-Na_xCoO_2 (Reproduced with permission.[33] Copyright 2011, Nature Publishing Group.), (c) O3-$NaMnO_2$, (Reproduced with permission.[37] Copyright 2011, The Electrochemical Society.), (d) P2-$Na_{0.6}MnO_2$ (Reproduced with permission.[36] Copyright 2002, Royal Society of Chemistry.), (e) O3-$NaFeO_2$, (Reproduced with permission.[44] Copyright 2012, The Electrochemical Society of Japan), (f) P2-$Na_xFe_{1/2}Mn_{1/2}O_2$ (Reproduced with permission.[46] Copyright 2012, Nature Publishing Group.), (g) O3-$NaNi_{0.5}Mn_{0.5}O_2$ (Reproduced with permission.[56] Copyright 2012, American Chemical Society), (h) P2-$Na_{2/3}Ni_{1/3}Mn_{2/3}O_2$ (Reproduced with permission.[61] Copyright 2001, The Electrochemical Society), (i) O3-$NaNi_{1/3}Mn_{1/3}Co_{1/3}O_2$ (Reproduced with permission.[57] Copyright 2012, American Chemical Society), (j) P2-$Na_{0.45}Ni_{0.22}Co_{0.11}Mn_{0.66}O_2$ (Reproduced with permission.[62] Copyright 2013, American Chemical Society), (k) O3-$NaNi_{1/3}Fe_{1/3}Mn_{1/3}O_2$. (Reproduced with permission.[58] Copyright 2012, Elsevier), (l) P2-$Na_{1.0}Li_{0.2}Ni_{0.25}Mn_{0.75}O_y$. (Reproduced with permission.[64] Copyright 2011, Wiley-VCH.)

1980s.[17,30] The structural change in Na_xCoO_2 was first studied by Delmas and co-workers.[30] The reversible phase transition of O3 → O′3 → P′3 was proposed for the initial O3-$NaCoO_2$ within a Na content range of $0.5 \leq x \leq 1$ (Fig. 4a). Recently, this group re-examined the complex structure evolution of P2-Na_xCoO_2 (Fig. 4b) through an *in situ* X-ray diffraction (XRD) experiment, which showed various single- or two-phase domains with different Na^+/V_{Na+} patterns depending on Na concentration with better accuracy compared with their previous studies.[33] The electronic conductivity of Na_xCoO_2 is always related to the preparation conditions (*e.g.* temperature, oxygen pressure). The relationship between the electronic and electrochemical properties of non-stoichiometric $Na_{0.7}CoO_{2-y}$ was also investigated.[34] Shacklette and co-workers investigated the series phases of O3, O′3, P3 and P2 Na_xCoO_2 bronzes, and determined that P2 phase offers better cycle life probably due to the gross structural stability during cycling.[35]

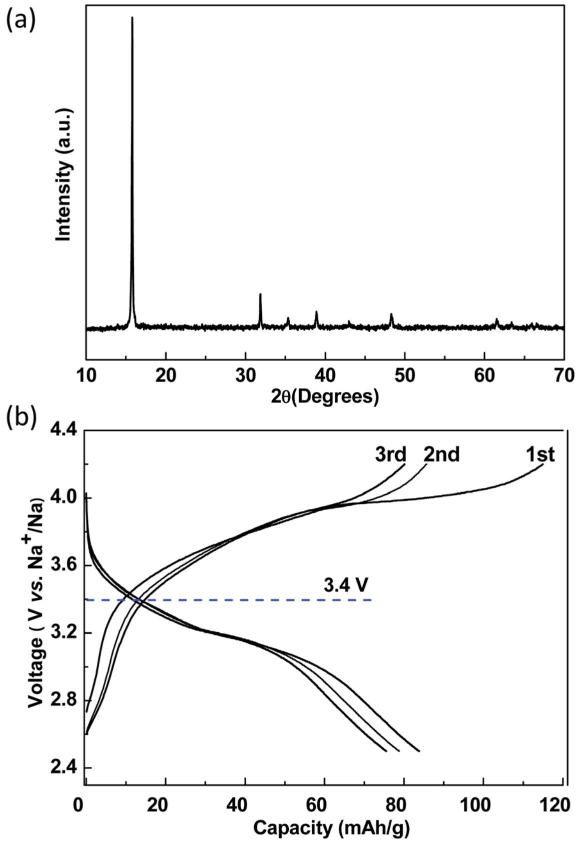

Fig. 5 (a) The XRD pattern of P2-$Na_{0.67}Fe_{0.67}Mn_{0.33}O_2$, (b) the charge–discharge curves of P2-$Na_{0.67}Fe_{0.67}Mn_{0.33}O_2$/Na at a current rate of 0.1C (2.5–4.2 V) in 1 M $NaClO_4$/EC : DEC electrolyte.

Na_xMnO_2 is another layered Na transition metal oxide that was investigated early on. Hagenmuller and co-workers first studied the Na–Mn–O ternary system in 1971, and determined the existence of several phases of Na_xMnO_2 within the range of $0 \leq x \leq 1$.[16] The P2-type $Na_{0.7}MnO_{2+y}$ exhibits a reversible capacity of approximately 100 mA h g^{-1} within the range of $0.45 \leq x \leq 0.85$, as reported by Hagenmuller's group.[31] P2-$Na_{0.6}MnO_2$ ($P6_3/mmc$) was also reported with a capacity of 140 mA h g^{-1} over the initial few cycles (Fig. 4d); however, its capacity decays in subsequent cycles.[36] Ceder's group recently reported that monoclinic α-$NaMnO_2$ ($C2/m$) exhibits a reversible capacity of 185 mA h g^{-1} (0.8 Na) in the first cycle in a voltage range of 2.0 V–3.8 V, as well as rapid capacity decay (Fig. 4c).[37] Unlike $LiMnO_2$, $NaMnO_2$ is free from the phase transition from a layered structure to a spinel during the initial cycles, resulting from the fact that Na^+ ions are too large for the tetrahedral sites occupation in a spinel.[38,39] Thus, the $NaMnO_2$ exhibits reversible capacity. The capacity decay for Na_xMnO_2 may be related to the instability of the structure in the presence of moisture and/or the strong Jahn–Teller effect of Mn^{3+}.[30,40] Substituting another TM element (*e.g.*, Ni^{2+}/TM^{4+}, Co^{3+}, Fe^{3+}, *etc.*) or an alkali ion (*e.g.*, Li^+, Mg^{2+}, *etc.*) for a quantity of Mn^{3+} may stabilize the structure of Na_xMnO_2 and enhance its cycle life as in the case of Li-ion batteries.[41,42] The other essential for layered Na_xMnO_2 electrode materials is to further improve the storage voltage of redox Mn^{4+}/Mn^{3+} before a practical application.

The O3-type α-$NaFeO_2$ ($R\bar{3}m$) has also attracted much attention for its inexpensive and non-toxic characteristics, and was expected to support reversible Fe^{4+}/Fe^{3+} conversion. A previous work shows that Na^+ ions could be removed and a new phase of $Na_{0.5}FeO_2$ could be formed with the removal of 0.4–0.5 Na per formula unit.[43] Recent studies present reversible Na storage in $NaFeO_2$ at 3.3 V with a small polarization by limiting the cut-off voltage (Fig. 4e).[44,45] In contrast, it should be noted that its Li analogue O3-$LiFeO_2$ is nearly inactive electrochemically on the basis of the Fe^{4+}/Fe^{3+}; the observed charge capacity in the half cell is ascribed to the dominant reaction of oxygen removal at the solid/electrolyte interface rather than Fe^{4+}/Fe^{3+} conversion because the Fe^{3+} 3d-orbital is strongly hybridized with the oxygen 2p orbital in the Li system; oxygen removal is more favorable than the oxidation to Fe^{4+}.[46] P2-$Na_{0.67}Fe_{0.5}Mn_{0.5}O_2$ (Fig. 4f) was also proposed to provide the reversible Fe^{4+}/Fe^{3+} conversion confirmed by the Mössbauer spectroscopy with a reversible capacity of 190 mA h g^{-1} (Note that part of reversible capacity (50 mA h g^{-1}) is compensated by the Na anode in the first discharge process), which is higher than that of O3-$NaFe_{0.5}Mn_{0.5}O_2$.[46] We recently also investigated sodium storage in P2-$Na_{0.67}Fe_{0.67}Mn_{0.33}O_2$ with Fe(III)/Mn(VI) = 2/1 in the TM layer. Approximately 0.44 Na can be extracted when charged to 4.2 V, and *ca.* 0.33 Na can be reversible during the discharge process, as shown in Fig. 5, which might correspond to the reversible conversion of Fe^{4+}/Fe^{3+}. Recently, Na storage properties for a series of $Na_xFe_xMn_{1-x}O_2$ ($0.5 < x < 1$) compounds were represented by Thorne *et al.*[47] The substitution of Mn for Fe was determined to result in a significant reduction in voltage hysteresis and increased capacity retention during cycling. The reversible reaction of Fe^{4+}/Fe^{3+} redox in Na containing compounds is an important finding, reminding us of designing electrode material with the Earth-abundant element Fe to realize Fe^{4+}/Fe^{3+} conversion in certain special structures.

$NaCrO_2$ ($R\bar{3}m$) has the same structure as $LiCrO_2$. However, their electrochemical storage performance differs remarkably. $NaCrO_2$ shows a reversible capacity of *ca.* 120 mA h g^{-1} (corresponding to *ca.* 0.5 Na) with satisfied capacity retention.[48–51] In contrast, its Li analogue $LiCrO_2$ is electrochemically inactive.[52] In $LiCrO_2$, Cr^{4+} tends to disproportionately transfer to Cr^{6+}

($3Cr^{4+} = 2Cr^{3+} + Cr^{6+}$) upon Li removal. The smaller sized Cr^{6+} can irreversibly migrate to the interstitial tetrahedral site in the Li layer, leading to poor reversibility. In the case of $NaCrO_2$, the resulting Cr^{4+} is more stable upon Na removal, which has been confirmed in the deintercalated $Na_{1-x}CrO_2$ by X-ray absorption analyses.[50] The larger Cr^{4+} (*vs.* Cr^{6+}) would stay in the TM layer, thus ensuring reversible Na storage.[49] The reason for the difference in charge transfer mechanisms between $LiCrO_2$ and $NaCrO_2$ upon alkali ion extraction remains unknown and needs further elucidation. The charge transfer mechanism and ionic size of the alkali ion in $ACrO_2$ would be responsible for the different electrochemical properties.

Monoclinic $NaNiO_2$ ($C2/m$) has been previously synthesized and electrochemically tested in a Na-ion battery.[53] However, only 0.2 Na could be extracted from this structure in previous work.[53,54] Ceder's group recently re-examined the Na storage properties of $NaNiO_2$ in a Na-ion battery. They reported that $NaNiO_2$ displays a reversible capacity of 123 mA h g^{-1} (*ca.* 0.52 Na) with acceptable capacity retention achieved by limiting the voltage within a range of 1.25–3.75 V.[55]

A solid-solution layered oxide with several different metal ions in the transition metal layer was also proposed recently. O3-$NaNi_{0.5}Mn_{0.5}O_2$ reported by Komaba's group exhibits a capacity of 105–125 mA h g^{-1} in a voltage range of 2.2–3.8 V (Fig. 4g). A large capacity of 185 mA h g^{-1} was obtained when charged to 4.5 V; however a rapid capacity decline was also demonstrated. A full cell with $NaNi_{0.5}Mn_{0.5}O_2$ as the cathode and hard carbon as the anode was constructed by this group and shows promising cyclic performance.[56] O3-$NaNi_{1/3}Mn_{1/3}Co_{1/3}O_2$ was also reported to exhibit reversible intercalation of 0.5 Na (120 mA h g^{-1}) in a voltage range of 2–3.75 V, with good cyclic performance (Fig. 4i). However, $NaNi_{1/3}Mn_{1/3}Co_{1/3}O_2$ is unstable in air, which limits its applications.[57] While O3-$NaNi_{1/3}Mn_{1/3}Fe_{1/3}O_2$ (Fig. 4k) was demonstrated to have stable structure maintenance with good cyclic performance.[58] Layered $NaNi_{0.5}Ti_{0.5}O_2$ also exhibits a large capacity of more than 100 mA h g^{-1} coupled with the Ni^{4+}/Ni^{2+} redox process.[59] P2-type $Na_{2/3}Co_{2/3}Mn_{1/3}O_2$ was investigated by Delmas and co-workers and displays a reversible 0.5 Na intercalation within a voltage range of 1.5–4 V, with only one voltage step at an ordered phase P2-$Na_{1/3}Co_{2/3}Mn_{1/3}O_2$. The authors speculated that the coexistence of Co^{3+} and Mn^{4+} in the slab prevents the Na^+/V_{Na+} ordering, thus avoiding the complex structure evolution as in the case of Na_xCoO_2.[60] Lu and Dahn demonstrated that P2-$Na_{2/3}Ni_{1/3}Mn_{2/3}O_2$ can be able to deliver a capacity as high as 160 mA h g^{-1}, with nearly all Na removed from the slab (Fig. 4h). However, the cycle life was unknown for P2-$Na_{2/3}Ni_{1/3}Mn_{2/3}O_2$.[61] P2-$Na_{0.45}Ni_{0.22}Co_{0.11}Mn_{0.66}O_2$ (Fig. 4j) and P2-$Na_{0.67}Ni_{0.15}Co_{0.2}Mn_{0.65}O_2$ exhibit a capacity of 135–141 mA h g^{-1} with moderate rate and good cyclic performance.[62,63] However, partial capacity delivered at *ca.* 2.3 V is compensated by the Na anode during the first discharge process.[62] Johnson's group recently proposed an important Li substituted layered P2-$Na_{1.0}Li_{0.2}Ni_{0.25}Mn_{0.75}O_y$ for Na-ion batteries (Fig. 4l). A small amount of Li in this material stabilizes the TM layer and minimizes site/charge ordering, thus exhibiting a reversible capacity of 100 mA h g^{-1} with a good rate capability and excellent cycle life as well as a sloping charge–discharge voltage profile.[64]

Oxides containing vanadium, such as NaV_6O_{15}, were also proposed as electrode materials for Na-ion batteries.[65] However, these compounds do not consist of Na, which is required to combine Na metal or pre-sodiated anodes in a full cell. Na_xVO_2 exhibits a capacity of 120 mA h g^{-1} in a voltage range of 1.2–2.5 V and better cyclic performance.[66] However, more than half of the capacity was delivered in a 1.5–1.7 V voltage range, which is too low for a practical application.

Among most O3- and P2-type layered oxides, repeatable reversible capacity of *ca.*120 mA h g^{-1} can be obtained for O3 phase compounds. The P2 phase seems to deliver a higher capacity and better cycle life in Na-ion batteries. This case may be attributed to the structural difference between O3 and P2 phases. The Na ion occupies a larger trigonal prismatic site in P2 phase than the octahedral site in O3 phase, thus Na ion transport in P2 phase could be faster than that in O3 phase. In addition, the phase transition from P2 to other phases is more difficult because of involving a rotation of MO_6 octahedra and the breaking of M–O bonds. P2 phase is expected to exhibit better cyclic performance owing to the lack of significant structural change. However, further investigation is needed to enhance structural stability and increase the capacity of P2-type electrodes from the viewpoint of practical applications. Therefore, determining the acceptable Na content range for the alkali ion layer in P2-type compounds is helpful in designing P2-type cathode with higher storage capacity. Furthermore, the composition and arrangement modification of the TM layer with an inactive element, such as Li^+, Mg^{2+}, Al^{3+}, Mn^{4+}, *etc.*, may stabilize the structure of the P2-phase. Several related works will be reported in our future publications.

2.2 Tunnel-type oxides

Orthorhombic $Na_{0.44}MnO_2$ (*Pbam*), first specified by Hagenmuller and co-workers in 1971, has a particular composition in the Na–Mn–O ternary system,[16] with a large S-shaped tunnel structure (Fig. 21c). However, this material was thought to suffer from a hopping mechanism difficulty, and thus the consequent electrochemical properties of this material were not measured.[16,31] Recently, many groups re-examined and proposed $Na_{0.44}MnO_2$ as a cathode material for Na-ion batteries because of its unique structure.[32,67–70] Doeff and co-workers first investigated the reversible Na storage in $Na_{0.44}MnO_2$ in a solid polymer electrolyte battery.[32] Baudrin *et al.* investigated the Na insertion/deinsertion mechanism in $Na_{0.44}MnO_2$ *via* an *in situ* XRD experiment, which revealed at least six distinct biphasic phenomena between 2 V and 3.8 V within a composition range of $0.18 \leq x \leq 0.64$ in Na_xMnO_2.[67] Cao *et al.* reported that $Na_{0.44}MnO_2$ ($Na_4Mn_9O_{18}$) nanowires (Fig. 6) prepared through a polymer pyrolysis method exhibit good rate capability and excellent cycle life with a capacity retention of 77% after 1000 cycles at 0.5C.[68] However, only *ca.* 0.22 Na can be reversibly cycled for $Na_{0.44}MnO_2$ in a full cell (Note that the other 0.22 Na is from the Na anode during the first discharge in a half cell.). The capacity of $Na_{0.44}MnO_2$ is too low for use in a practical non-aqueous battery.

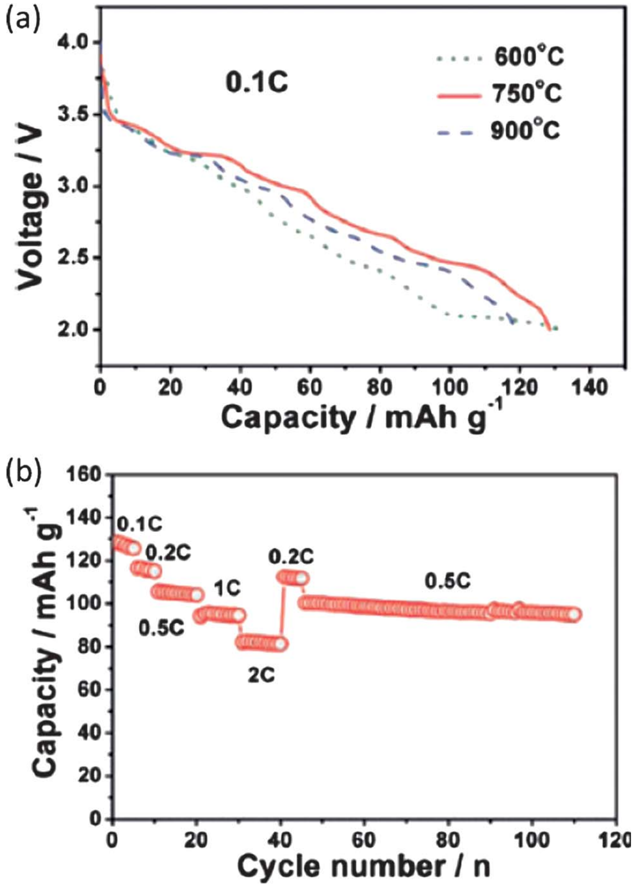

Fig. 6 (a) The typical charge–discharge profiles of $Na_{0.44}MnO_2$ nanowires calcined at different temperatures, (b) the rate and cyclic capability of $Na_{0.44}MnO_2$. (Reproduced with permission.[68] Copyright 2011, Wiley-VCH.)

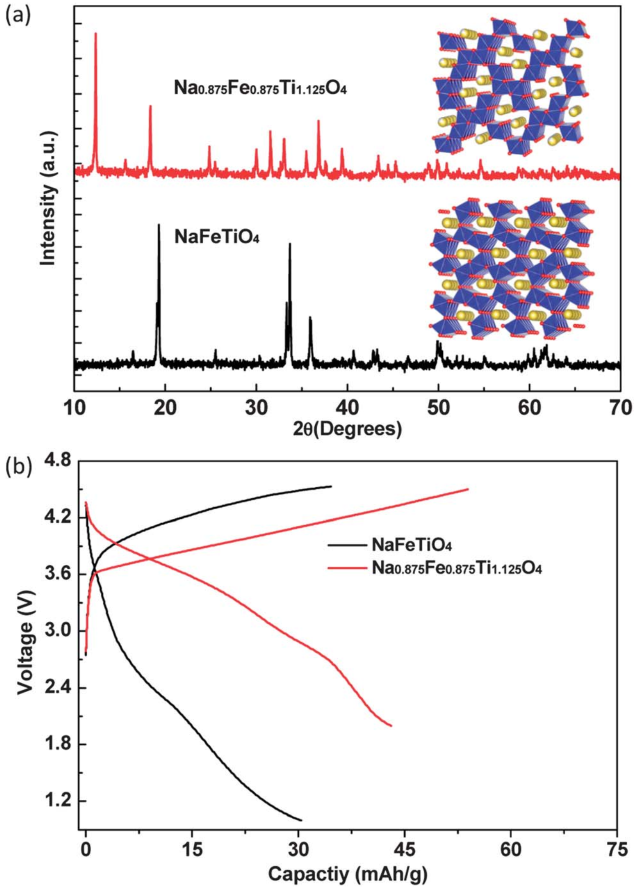

Fig. 7 (a) The XRD patterns of $Na_xFe_xTi_{2-x}O_4$ ($x = 1$, 0.875), (b) the Na storage properties of $Na_xFe_xTi_{2-x}O_4$ in half cells.

We have recently prepared another tunnel type $Na_xFe_xTi_{2-x}O_4$ ($x = 1$, 0.875) with the *Pnma* space group (Fig. 7a). However, only *ca.* 0.24 Na can be electrochemically extracted from this structure when charged up to 4.5 V, which might refer to the Fe^{4+}/Fe^{3+} redox in $NaFeTiO_4$ as shown in Fig. 7b. $Na_xFe_xTi_{2-x}O_4$ with a lower Na content appears to exhibit better kinetics during Na extraction when charged to 4.5 V, *ca.* 0.37 Na can be extracted from $Na_{0.875}Fe_{0.875}Ti_{1.125}O_4$ with smaller polarization, which may be associated with higher conductivity resulting from increased Na vacancies and/or suitable transport channel.[71] A higher amount of Na is expected to be further extracted if charged to a higher voltage employing a stable electrolyte with a wider voltage window. This result is consistent with the chemically desodiation results that *ca.* 0.44 Na can be extracted from $Na_{0.875}Fe_{0.875}Ti_{1.125}O_4$ by using NO_2BF_4 as an oxidation agent.[71] In addition, it should be emphasized that this tunnel-type oxide offers a stable structure to accommodate Fe^{4+} compared with layered oxides (*e.g.*, α-$NaFeO_2$).[43]

2.3 Phosphates

Phosphates have attracted much attention in Li-ion batteries, because of their structural and thermal stability and the higher redox potential of TMs resulting from the inductive effect of PO_4^{3-} polyanion.[72,73] Work on Na phosphates for Na-ion batteries was also reported by many groups.[74–126]

2.3.1 Olivine $NaMPO_4$ (M = Fe, Mn, *etc.*). The thermodynamically stable structure of $NaFePO_4$ is not olivine, but maricite, in which the sites for Na^+ and Fe^{2+} are just the opposite of those in olivine $LiMPO_4$.[74] $NaMPO_4$ (M = Fe, Mn, Co, *etc.*) prepared through a normal route with a maricite structure that is electrochemically inactive because of the lack of cationic transport channel in the structure.[75–77] Recently, olivine $NaFePO_4$ was obtained through electrochemical Na insertion into heterosite $FePO_4$ which can be obtained from chemical or electrochemical delithiation of olivine $LiFePO_4$.[78] Unlike $LiFePO_4$, the olivine $NaFePO_4$ exhibits an intermediate phase of $Na_{0.7}FePO_4$ at 2.95 V during the charge process with good cycle life (Fig. 8a). Amorphous $FePO_4$ was also reported to store Na with a capacity of 66–100 mA h g^{-1}.[79–81] Nazar and co-workers prepared olivine $NaMn_xM_{1-x}PO_4$ (M = Fe, Ca, Mg) by a topotactic reaction that converts the precursor $NH_4Mn_xM_{1-x}PO_4 \cdot H_2O$ to $NaMn_xM_{1-x}PO_4$. In contrast to olivine $NaFePO_4$ or $LiFePO_4$, the charge–discharge profiles of the olivine $NaMn_{0.5}Fe_{0.5}PO_4$ electrode display a sloping behavior (Fig. 8b); it is not clear whether this suggests a single-phase reaction or is related to the kinetics limitation.[82] The electrochemical activity of $NaMn_xFe_{1-x}PO_4$ seems to decrease as the Mn content is increased, which is similar to the case of

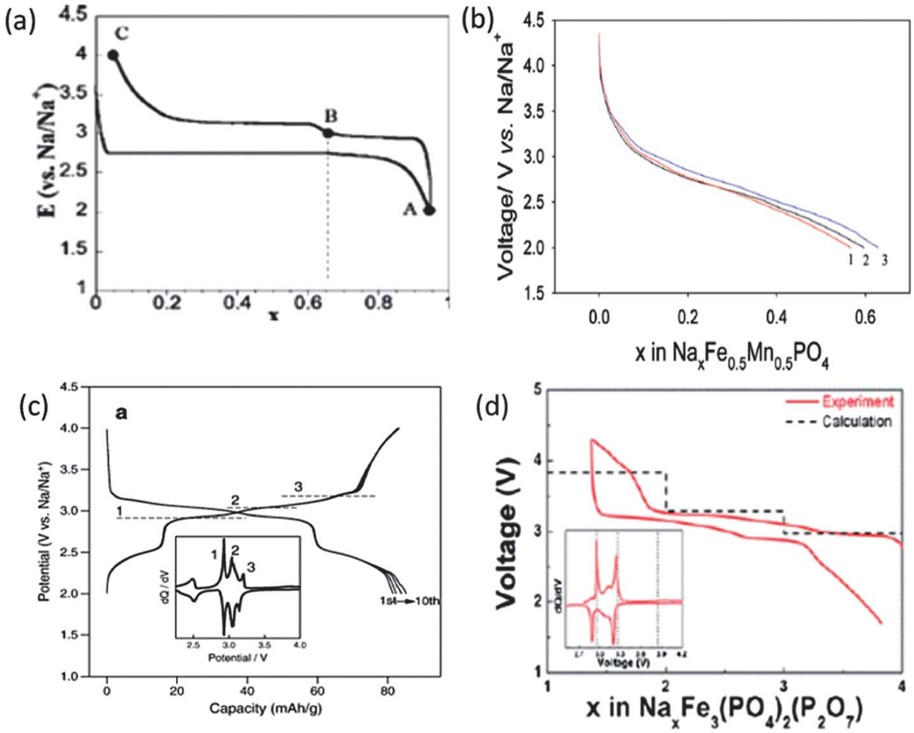

Fig. 8 The charge–discharge profiles of various phosphates. (a) $NaFePO_4$ (Reproduced with permission.[78] Copyright 2010, American Chemical Society), (b) $NaFe_{0.5}Mn_{0.5}PO_4$ (Reproduced with permission.[82] Copyright 2011, American Chemical Society), (c) $Na_2FeP_2O_7$ (Reproduced with permission.[84] Copyright 2012, Elsevier.), (d) $Na_4M_3(PO_4)_2P_2O_7$ (Reproduced with permission.[90] Copyright 2012, American Chemical Society.)

$LiMn_{1-x}Fe_xPO_4$, thus indicating the unfavorable kinetics of Mn in phosphate.[83]

2.3.2 Pyrophosphates and mixed polyanions.

Yamada's group first reported a triclinic pyrophosphate $Na_2FeP_2O_7$ ($P1$) exhibiting a reversible capacity of 83 mA h g^{-1} at around 3 V associated with Fe^{3+}/Fe^{2+} redox (Fig. 8c).[84] Recently $Na_{2-x}Fe_{1+x/2}P_2O_7$/C composites ($x = 0$–0.44) prepared by Honma *et al.* through a glass-ceramic process exhibited high rate and good cyclic performances.[85] The Na storage mechanism and thermal stability of $Na_2FeP_2O_7$ were also investigated by Choi *et al.* through an *ex situ* XRD, and thermogravimetry/differential thermal analysis (TG/DTA) measurements, which revealed both single- and two-phase reactions.[86] In addition, pyrophosphate $Na_2CoP_2O_7$ ($Pna2_1$) with a layered structure and triclinic $Na_2MnP_2O_7$ (P1) were investigated for Na-ion batteries by Yamada's group, and they found shows a sloping voltage profile with an average voltage of 3 V and 3.65 V, respectively.[87,88] A series of pyrophosphates of $Na_2MP_2O_7$ (M = Mn, Co, Fe, *etc.*) should be further explored for a comprehensive understanding of pyrophosphates in Na-ion batteries as well as the reaction mechanism. The Fe^{3+}/Fe^{2+} redox couple in mixed polyanion groups of $PO_4{}^{3-}$ and $P_2O_7{}^{4-}$ was also initially proposed by Kang's group recently in the case of $Na_4Fe_3(PO_4)_2P_2O_7$. $Na_4Fe_3(PO_4)_2P_2O_7$ belongs to a known mixed polyanion $Na_4M_3(PO_4)_2P_2O_7$ (M = Co, Ni, Mn, Mg, *etc.*), which is composed of a three-dimensional (3-D) network of $[M_3P_2O_{13}]_\infty$ finite layer parallel to the *b*–*c* plane.[89] $Na_4Fe_3(PO_4)_2P_2O_7$ shows a capacity of *ca.* 110 mA h g^{-1} with an average voltage of 3.2 V at a current rate of C/40 (Fig. 8d).[90] The potential for Fe^{3+}/Fe^{2+} redox in this mixed polyanion compound is higher than that in phosphates and pyrophosphates, which provides a new family for Na accommodation in Na-ion batteries. However, the Mn^{2+} and Ni^{2+} in this structure seem to be nearly inactive electrochemically when charged to 4.6 V *vs.* Na^+/Na in our recent work. This outcome may be attributed to the sluggish kinetics or much higher redox potential of Mn^{2+} and Ni^{2+} beyond the stability range of present electrolytes.

2.3.3 NASICON $Na_xM_2(PO_4)_3$.

NASICON (Na Super Ionic Conductor) type compounds were originally proposed by Hong and Goodenough as Na^+ ion solid electrolytes due to the high Na^+ ionic conductivity related to their 3-D open framework.[91,92] NASICON compounds can also be used as electrode materials with TM in this structure; however, such investigations are rare. Redox couples of TMs (*e.g.*, V^{4+}/V^{3+}, V^{3+}/V^{2+}, Fe^{3+}/Fe^{2+}, Ti^{4+}/Ti^{3+}, Nb^{5+}/Nb^{4+}, Nb^{4+}/Nb^{3+}) in NASICON phosphates for Li intercalation were first investigated by Goodenough.[93] A typical NASICON material of $Na_3V_2(PO_4)_3$ was initially synthesized by Delmas and co-workers.[94] Different from $Li_3V_2(PO_4)_3$ ($P2_1/c$), the structure of $Na_3V_2(PO_4)_3$ ($R\bar{3}c$) can be regarded as each VO_6 octahedron corner sharing with three PO_4 tetrahedrons, and one Na^+ ion occupying in the M1 (6b) site and the other two in the M2 (18e) site of the interstitial sites, where M1 sites are situated between two adjacent $[V_2(PO_4)_3]$ units in the same $[V_2(PO_4)_3]_\infty$ ribbon while M2 sites are located between adjacent $[V_2(PO_4)_3]\infty$ ribbons (Fig. 21f).[95] Yamaki and co-workers first reported the Na storage properties of pure $Na_3V_2(PO_4)_3$, which delivers a reversible capacity of 140 mA h g^{-1} in a voltage range of 1.2–3.5 V associated with the V^{4+}/V^{3+}, V^{3+}/V^{2+} redox couples, 90 mA h g^{-1} of which is from the V^{4+}/V^{3+} conversion.[96] Based on this, the same group, some years later, constructed a symmetric cell using $Na_3V_2(PO_4)_3$ as both cathode and anode. The cell exhibits an operated voltage of *ca.* 1.6 V, but with poor reversibility and cycle life.[97] Recently, Hu *et al.* proposed for the first time the use of carbon coating to significantly improve electrochemical Na storage performance in $Na_3V_2(PO_4)_3$, with a capacity of 93 mA h g^{-1} and a flat voltage plateau of 3.4 V *vs.* Na^+/Na in 1 M $NaClO_4$/PC electrolyte.[95] However, the coulombic efficiency cannot be increased because of the side reaction between the used electrolyte and the electrodes. The electrolyte was further optimized to enhance the electrode stability in our recent investigation.[98] The initial coulombic efficiency can reach as high as 98.7% with a reversible capacity of 107 mA h g^{-1}, and can be maintained at 99.8% in subsequent cycles in 1 M NaFSI/PC electrolyte with excellent cyclic stability. $Na_3V_2(PO_4)_3$ also exhibits significantly improved coulombic efficiency in 1 M $NaBF_4$/PC, $NaPF_6$/EC : DEC and NaFSI/EC : DEC compared with $NaClO_4$/PC electrolyte in half cells. The structural evolution was also examined *via in situ* XRD measurement, which exhibits a typical two-phase reaction between $Na_3V_2(PO_4)_3$ and $NaV_2(PO_4)_3$ (Fig. 9). The volume change between them is only 8.26%, which is similar to $LiFePO_4$ (~7%).[99] A full cell using hard carbon as anode and $Na_3V_2(PO_4)_3$ as cathode exhibits an average operating voltage of 2.7 V with a theoretical energy density of *ca.* 180 W h kg^{-1}. Research on Na occupancy and diffusion in $Na_3V_2(PO_4)_3$ by nuclear magnetic resonance (NMR) measurements is on-going in our group. Kim's and Balaya's groups investigated porous $Na_3V_2(PO_4)_3$/C composite, which shows significantly improved rate and cyclic performance.[100,101] Choi investigated thermal stability of the desodiated state of $Na_3V_2(PO_4)_3$ by TG/DSC and *in situ* XRD, and determined that the $NaV_2(PO_4)_3$ phase could maintain stability up to 450 °C.[102] $Na_3V_2(PO_4)_3$, with good electrochemical and thermal stability as well as long cycle life, exhibits promising applications in rechargeable Na-ion batteries.

Although NASICON-type $Na_3V_2(PO_4)_3$ shows promise in terms of applications, obtaining electrode materials using non-toxic and Earth-abundant active elements remains essential. If the redox couples, such as Fe^{3+}/Fe^{2+}, $Mn^{4+}/Mn^{3+}/Mn^{2+}$ and Ni^{4+}/Ni^{2+} could be reversibly realized in NASICON-type compounds for Na-ion batteries, it would attract more interest and would be more important. However, investigations have rarely been conducted to date. $Na_3Fe_2(PO_4)_3$ exists as a NASICON compound, but $Na_3Fe_2(PO_4)_3$ can only accommodate no more than one Na into a formula unit, with a capacity of *ca.* 45 mA h g^{-1}, due to full occupancy at Na sites after one Na insertion.[94] The conversion voltage from Fe^{3+} to Fe^{2+} in $Na_3Fe_2(PO_4)_3$ is *ca.* 2.5 V *vs.* Na^+/Na, which is too low to be used as a cathode. The conversion from Fe^{2+} to Fe^{3+} always exhibits higher voltage than that from Fe^{3+} to Fe^{2+} in phosphates.[93] Divalent ions (*e.g.*, Ca^{2+}, Mg^{2+}, Sr^{2+}, *etc.*) can occupy the Na^+ site in many NASICON compounds.[103] Thus, $Na_3CaM_2(\text{II})(PO_4)_3(M = Fe, Mn \text{ and } Ni)$ with full occupancy at the Na site was designed as a NASICON-type cathode material in our early expectation. Unfortunately, all attempts to synthesize these compounds failed. This outcome could be attributed to divalent ion substitution of Na^+ in the aforementioned NASICON compound which leads to structure degradation from NASICON ($R\bar{3}c$) to alluaudite ($C2/c$).[104,105] The Na site in alluaudite could not accommodate 4 Na, thus $Na_3CaM_2(\text{II})(PO_4)_3$ could not be synthesized in our experiments. $Na_3Mn(\text{II})Zr(PO_4)_3$ and $Na_3Ni(\text{II})Zr(PO_4)_3$ are known as NASICON-type compounds, including Mn^{2+} and Ni^{2+}.[106,107] We synthesized phase-pure $Na_3MnZr(PO_4)_3$ and

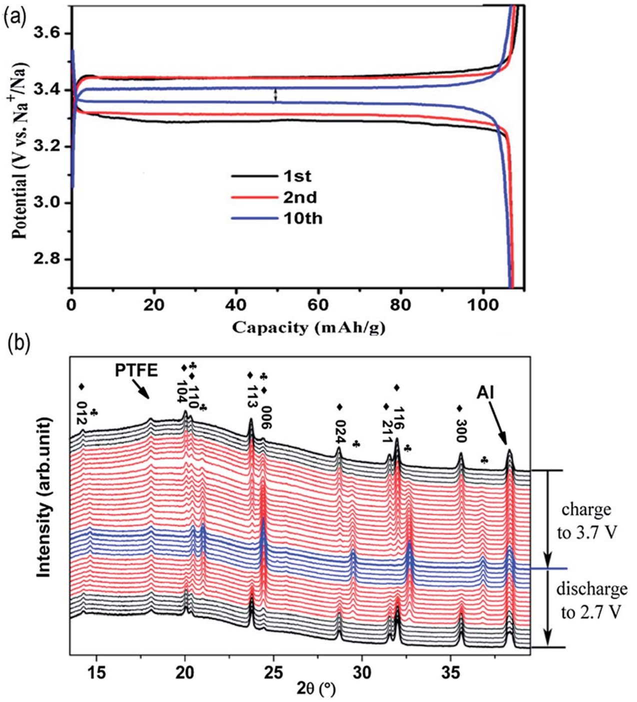

Fig. 9 (a) The 1st, 2nd and 10th charge–discharge curves of $Na_3V_2(PO_4)_3$/C electrodes in NaFSI/PC electrolyte; (b) *in situ* XRD patterns of $Na_3V_2(PO_4)_3$/Na cell. (Reproduced with permission.[98] Copyright 2013, Wiley-VCH.)

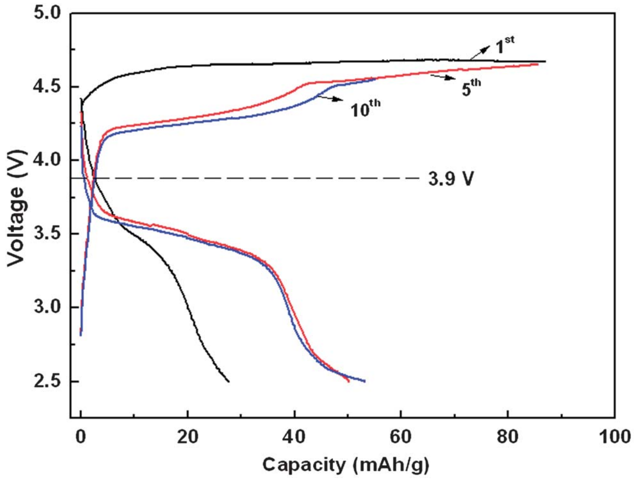

Fig. 10 The 1st, 5th and 10th charge–discharge profiles of the $Na_3NiZr(PO_4)_3$/Na batteries.

$Na_3NiZr(PO_4)_3$ through a solid-sate approach and also tested their electrochemical properties in Na-ion batteries. The $Na_3MnZr(PO_4)_3$ is nearly inactive electrochemically, which may be attributed to its poor kinetics or the instability of Mn^{3+} after Na extraction. Approximately one Na can be extracted from $Na_3NiZr(PO_4)_3$. However, the initial charge exhibits obvious electrolyte decomposition above the electrolyte voltage window, which shows a clear activation process, a large polarization of *ca.* 0.8 V and an average potential of 3.9 V *vs.* Na^+/Na associated with Ni^{3+}/Ni^{2+} (Fig. 10). Further optimization, including nanosizing or carbon coating, may help improve Na storage performance. Their derivatives, such as $Na_3Mn(\text{II})Ti(PO_4)_3$, $Na_3Ni(\text{II})Ti(PO_4)_3$ and $Na_3Ni(\text{II})Mn(\text{IV})(PO_4)_3$, were also designed as cathode materials. All trials failed.

Besides these, NASICON-type $NaTi_2(PO_4)_3$ exhibits a reversible Na storage capacity of *ca.* 120 mA h g^{-1} at *ca.* 2.1 V *vs.* Na^+/Na *via* Ti^{4+}/Ti^{3+} conversion, which could be used as an anode in the aqueous Na-ion batteries.[108,109] Ti^{3+}/Ti^{2+} and Ti^{4+}/Ti^{3+} redox conversions were recently reported in NASICON $Na_3Ti_2(PO_4)_3$, which is similar to the case of V^{4+}/V^{3+} and V^{3+}/V^{2+} conversions in $Na_3V_2(PO_4)_3$,[95] but is rarely seen in other structures for Ti.[110]

2.3.4 Alluaudites. Phosphates of the alluaudite group are accessory minerals in granitic pegmatite. The structure of a natural alluaudite sample was first reported by Moore in 1971.[111] The alluaudite is monoclinic with the *C*2/*c* space group and the structural formula of $[A(2)A(2)'][A(1)A(1)'A(1)'']M(1)M(2)_2(PO_4)_3$. Its structure consists of infinite chains formed by a succession of M(2) octahedral pairs linked by a highly distorted M(1) octahedral; the equivalent chains are connected by phosphate tetrahedral, in which the M sites must be filled and the A sites (always alkaline ions) in the tunnel can either be empty or partially filled.[112] Obvious Na channels were observed in the alluaudite structure, which seems interesting for alkaline ion insertion/extraction into/from A sites. Delmas and co-workers investigated the electrochemical properties of alluaudite $NaMnFe_2(PO_4)_3$, and found that the polarization is quite large during redox reactions. The alluaudites $Li_{0.5}Na_{0.5}MnFe_2(PO_4)_3$ and $NaFe_3(PO_4)_3$ both exhibit poor Li/Na storage properties,[113,114] which could be ascribed to the difficult electron transfer or the one-dimensional (1-D) alkaline diffusion characteristics. Reducing the particle size of alluaudite or carbon coating could be an effective means of improving their electrochemical properties.

2.3.5 Fluorophosphates. Combining F^- ions with phosphates results in a new class of structural host and compositions. Recently, many fluorophosphates have been described as new cathodes for both Li- and Na-ion batteries.[115,116] Na vanadium fluorophosphate $Na_3V_2(PO_4)_2F_3$, which was first demonstrated by Barker *et al.*, exhibits promising storage properties in a hybrid cell.[117] Recently, this compound was also investigated in a Na-ion battery by Kang's group, exhibiting two plateaus at *ca.* 3.7 V and 4.2 V, and a high capacity of 120 mA h g^{-1} (Fig. 11a).[118] The $Na_3V_2(PO_4)_2F_3$ exhibits the highest average voltage of 3.95 V among all cathode materials with the redox couple V^{4+}/V^{3+}. $NaVPO_4F$ (82 mA h g^{-1}), $NaV_{1-x}Cr_xPO_4F$ (75–87 mA h g^{-1}) and $Na_{1.5}VOPO_4F_{0.5}$ (87 mA h g^{-1}) all show attractive Na storage properties in a relatively high voltage range of 3–4.5 V, aside from a slightly low storage capacity (Fig. 11b).[119–121] Recently, a series of $Na_3V_2O_{2x}(PO_4)_2F_{3-2x}$ ($0 \le x \le 1$) materials have been investigated for their Na storage properties, exhibiting two plateaus at 3.6 V and 4.1 V *vs.* Na^+/Na with a capacity of 84–106 mA h g^{-1} in 2.5–4.3 V voltage range.[122,123] Nazar and co-workers originally proposed Na_2MPO_4F (M = Fe, Mn, Co, Ni) and $Na_2Fe_xM_{1-x}PO_4F$ and investigated the structure and electrochemical properties in a hybrid cell.[124] Recent studies indicate that carbon-coated Na_2FePO_4F (Fig. 11c) and $Na_2Fe_{0.5}Mn_{0.5}PO_4F$ deliver a reversible capacity of 110 mA h g^{-1} associated with the Fe^{3+}/Fe^{2+} (3.0 V *vs.* Na^+/Na) and Mn^{3+}/Mn^{2+} (3.53 V *vs.* Na^+/Na), and good rate capability in Na-ion batteries.[116,125] While the Na_2MnPO_4F with a $P2_1/n$ space group exhibits poor electrochemical activity. Kang and co-workers investigated the Na^+ ion diffusion kinetics and their studies show an acceptable activation barrier of 400–600 meV for Na_2MnPO_4F through different migration paths. Nano-sized Na_2MnPO_4F sample, which was also prepared by Kang's group, exhibits a reversible capacity of 120 mA h g^{-1} within a voltage range of 1–4.8 V, but with poor capacity retention.[126] Although many fluorophosphate cathodes exhibit promising Na storage performance, an environmental issue of the possible release of fluorine gas might be involved when these components are produced on a large-scale.

2.4 Fluorides

Perovskite transition metal fluorides MF_3 and $NaMF_3$ (M = Ni, Fe, Mn) were investigated as electrode materials for sodium-ion batteries, in which FeF_3 and $NaFeF_3$ were mostly investigated. Ball-milled FeF_3/C composite delivers an initial discharge capacity of 150 mA h g^{-1} associated with the Fe^{3+}/Fe^{2+} conversion.[127] $NaFeF_3$ exhibits an initial high reversible capacity of 197 mA h g^{-1} in a voltage range of 1.5–4 V.[128] However, the polarization is always quite large for these fluorides because of the poor kinetics, thus leading to a low energy conversion efficiency that limits their practical applications.

2.5 Hexacyanoferrates

Prussian blue $KFeFe(CN)_6$ is a prototype transition metal hexacyanoferrate with an open framework. In recent years, its analogues have been investigated as an electrode material for rechargeable batteries.[129–133] Cui's group reported the excellent electrochemical properties of $K_xCuFe(CN)_6$ and $K_xNiFe(CN)_6$ with K^+ or Na^+ insertion/extraction in an aqueous battery (Fig. 12a), exhibiting promise for application in large-scale ESS.[129–131] Prussian blue and its analogues $A_xMFe(CN)_6$ (A = K, Na; M = Ni, Cu, Fe, Mn, Co and Zn) have also been investigated as cathodes for sodium-ion batteries in organic electrolyte systems by Goodenough and co-workers (Fig. 12b), and were found to exhibit good rate and cyclic performance with the reversible conversion of $Fe(CN)_6{}^{3-}/Fe(CN)_6{}^{4-}$.[132,133] Yang's group reported another nano-sized $Na_4Fe(CN)_6$/C composite which shows a capacity of *ca.* 90 mA h g^{-1} at a high voltage of 3.4 V *vs.* Na^+/Na with a good rate kinetics (Fig. 12c).[134] Although these compounds present excellent electrochemical properties and non-toxicity themselves as well as low-cost, whether the

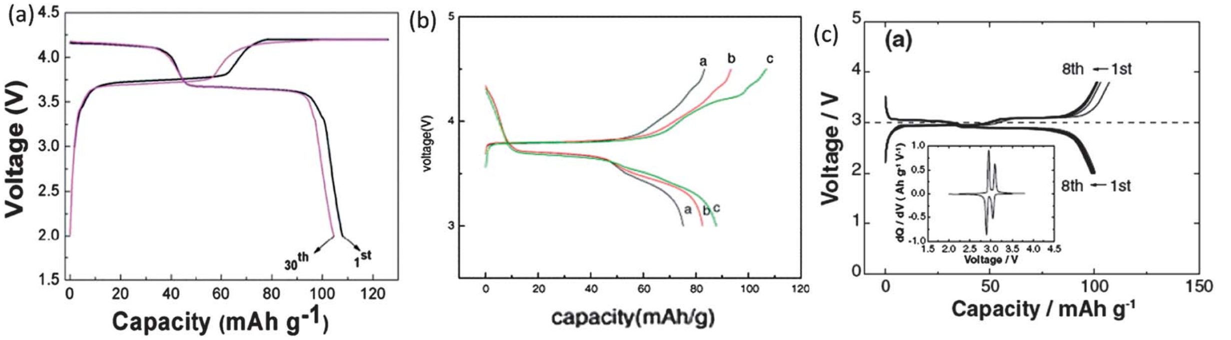

Fig. 11 The charge–discharge profiles of fluorophosphates, (a) $Na_3V_2(PO_4)_2F_3$ (Reproduced with permission.[118] Copyright 2012, Royal Society of Chemistry.), (b) $NaV_{1-x}Cr_xPO_4F$ (Reproduced with permission.[121] Copyright 2006, Elsevier.), (c) Na_2FePO_4F. (Reproduced with permission.[116] Copyright 2012, The Electrochemical Society of Japan.)

processes of producing them or their precursors involve an environmental issue remains unclear. The other issue is difficult to control the water content during synthesis which greatly influences the storage performance.

2.6 Organic compounds

Organic electrode materials, which can be obtained from natural biomass with minimum energy consumption, are environmentally-friendly and low-cost choices for future batteries.[135,136] Nevertheless, successful investigations of organic electrode materials are limited because of the high solubility of organic electrodes in organic liquid electrolytes, low thermal stability and sluggish kinetics, particularly poor electronic conductivity, whether in Li- or Na-ion batteries.[137] Ratnakumar *et al.* investigated organic tetracyanoethylene (TCNE) (Fig. 13a) in a high temperature (230 °C) Na-ion battery; however, energy density decreases rapidly with increasing TCNE concentration in the cathode because of the sluggish kinetics.[138] Several groups recently proposed organic radical polymers as novel cathodes in Na-ion batteries, with a doping–dedoping reaction with anions from the electrolyte noted by some groups.[139,140] Aniline–nitroaniline copolymer (Fig. 13b), reported recently by Yang's group, delivers a reversible capacity of 180 mA h g^{-1} at an average voltage of *ca.* 3.2 V *vs.* Na^+/Na with good capacity retention, thus exhibiting a promising application.[139] In addition, Kaskel *et al.* reported that a bipolar porous organic electrode (BPOE) constituted of aromatic rings in a porous-honeycomb structure exhibits 3.3 V and 2.3 V *vs.* Na^+/Na with p-type and n-type doping process.[141]

3 Anode materials

Graphite, which is the most commonly used anode material in Li-ion batteries, has a moderate Li storage capacity (~350 mA h g^{-1}) at approximately 0.1 V *vs.* Li^+/Li. Recent studies indicate that Na cannot be inserted into the graphite layer. This phenomenon might be related to thermodynamic issues.[142,143] To date, very few anode materials have been reported as viable. Unlike Li metal, Na metal is not a good choice because of its high reactivity and unstable passivation layer in most organic electrolytes at room temperature. Thus, identifying an anode with a proper Na storage voltage, large reversible capacity and high structural stability is urgently needed for the development of Na-ion batteries.

3.1 Carbon-based compounds

In 1993, Doeff first examined the Na storage behaviors in various carbon materials with PEO-$NaCF_3SO_3$ polymer as the electrolyte. Approximate compositions of NaC_{70}, NaC_{30} and NaC_{15} were formed for graphite, petroleum coke and Shawinigan black, respectively (Fig. 14a).[144] In 2000, Stevens and Dahn compared the electrochemical behavior of Li and Na storage in hard carbon produced from a glucose precursor.[145] They found that hard carbon exhibits a high reversible capacity of 300 mA h

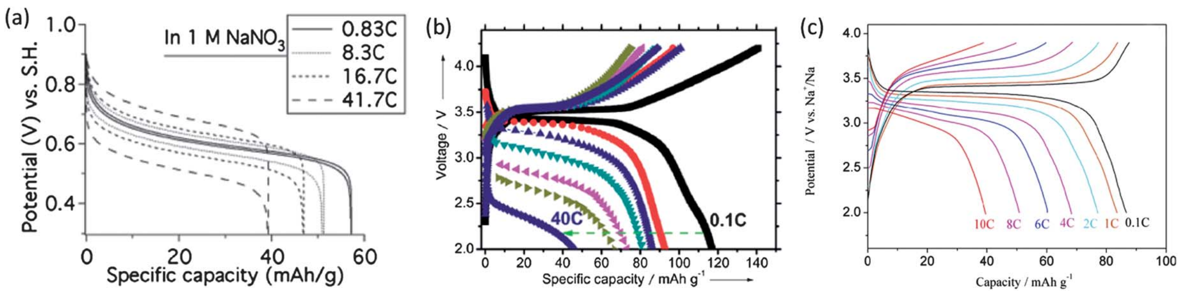

Fig. 12 (a) The potential profiles of (a) $K_{0.6}Ni_{1.2}Fe(CN)_6$ (Reproduced with permission.[130] Copyright 2011, American Chemical Society), (b) $Na_{1.72}MnFe(CN)_6$ (Reproduced with permission.[133] Copyright 2013, Wiley-VCH.), (c) $Na_4Fe(CN)_6$ (Reproduced with permission.[134] Copyright 2013, Wiley-VCH.).

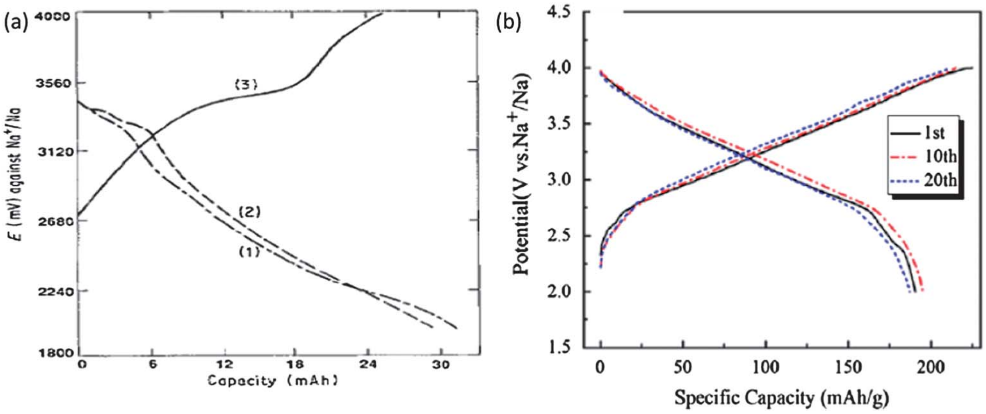

Fig. 13 The Na storage properties of organic electrodes. (a) Na/BASE/TCNE in $NaAlCl_4$ (Reproduced with permission.[138] Copyright 1990, Springer.); (b) aniline/nitroaniline copolymer (Reproduced with permission.[139] Copyright 2012, Elsevier).

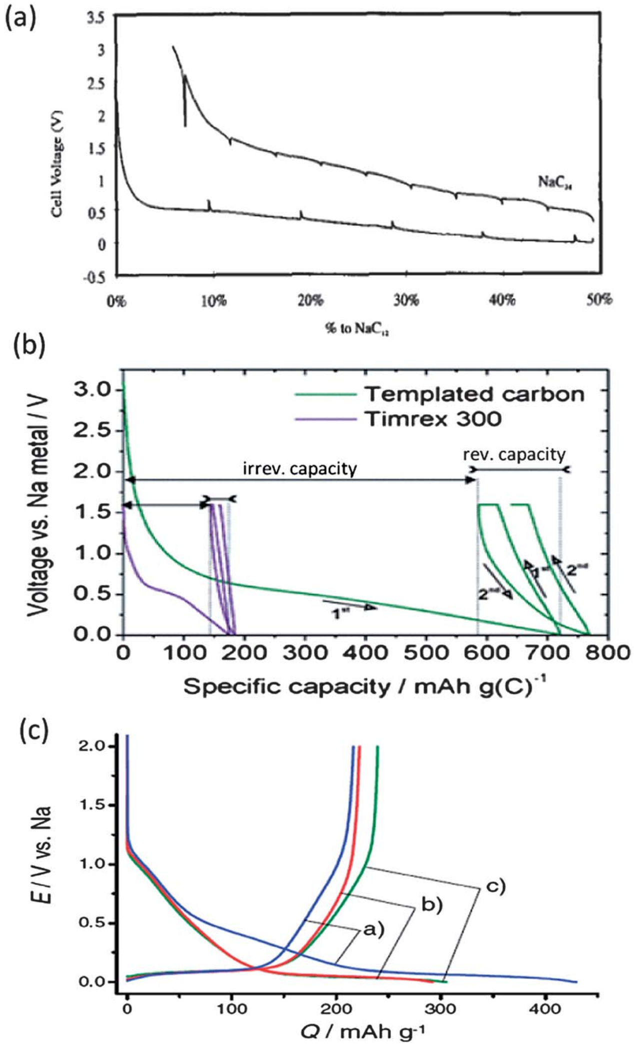

Fig. 14 The charge–discharge profiles various carbons. (a) petroleum coke (soft carbon) (Reproduced with permission.[144] Copyright 1993, The Electrochemical Society.), (b) hierarchical porous carbon. (Reproduced with permission.[148] Copyright 2012, Royal Society of Chemistry.) (c) Hard carbon (Reproduced with permission.[152] Copyright 2012, Wiley-VCH).

g^{-1} in a Na-ion battery and a metal insertion behavior which appears similar to that in a Li-ion battery, including a sloping region and a low-voltage region, which can be attributed to the insertion of Na or Li between parallel layers and into nano-pores between randomly stacked layers, respectively. This prediction has recently been confirmed by NMR study for the electrochemically inserted Na in hard carbon.[146] Billaud *et al.* reported that the electrochemical insertion of Na into hard carbon is associated with the carbon precursor and manufacturing process. In addition, the amount of Na insertion decreases when heat treatment temperature is increased.[147]

To date, numerous carbon materials with various morphologies, such as tailor-made carbon with hierarchical porosity (Fig. 14b),[148] hollow carbon nanospheres,[149] nanowires[150] and N-doped porous carbon nanosheets,[151] have been proposed for Na-ion batteries and display significantly improved storage performance and kinetics. However, their initial and subsequent coulombic efficiencies as well as cyclic stability cannot satisfy the requirement of practical application because of the side reaction related to the larger surface area resulting from the nanostructures. Komaba *et al.* re-examined hard carbon in various electrolytes, and found that the hard carbon exhibits initial capacity of 240 mA h g^{-1} in a voltage range of 0–2 V with an initial coulombic efficiency above 78% in 1 M $NaClO_4$/EC : DEC (1 : 1 by volume) electrolyte (Fig. 14c). They also determined that the reversible capacity and capacity retention of hard carbon anodes were dependent on the limited voltage range. A full cell based on a $NaNi_{0.5}Mn_{0.5}O_2$ cathode and hard carbon anode exhibits good cyclic stability in 1–3.5 V.[152] Nevertheless, the cost for hard carbon preparation is relatively high for commercial applications. If low-cost soft carbon, such as coke and bitumen, can work well in Na-ion batteries, this could be more attractive.

3.2 Oxides and sulfides

Most oxides can accommodate Li as anode material with high storage capacity; however, the case is not optimistic in Na-ion batteries, which may be due to the large size of Na^+ ion. $NiCo_2O_4$ spinel exhibits a reversible capacity of 200 mA h g^{-1} through a conversion reaction mechanism, however the initial coulombic efficiency of 35% is rather low.[153] Fu's group also reported a Sb_2O_4 thin film with a high reversible capacity of 896 mA h g^{-1} at a low current rate of C/70 in a voltage range of 0–3.5 V, but with large polarization between charge and discharge.[154] Komaba *et al.* reported that nano-crystalline Fe_3O_4 and α-Fe_2O_3 (*ca.* 10 nm) and hollow γ-Fe_2O_3 nanoparticles (*ca.*13.6 nm in diameter with *ca.* 3.3 nm thickness) have been investigated as hosts for Na with a rechargeable capacity of 160–189 mA h g^{-1} in a voltage range of 1–4 or 1.1–4 V, and with moderate capacity retention,[155,156] however such small-particle materials would lead to a lower volumetric energy density. Ti^{4+}/Ti^{3+} redox couple is highly reversible in lithium-ion batteries (*e.g.*, $Li_4Ti_5O_{12}$ (ref. 157 and 158)), and has also attracted a great deal of attention in Na-ion batteries. Palacín and co-workers reported that $Na_2Ti_3O_7$ can uptake 2 Na in a formula unit at a rather low voltage of 0.3 V *vs.* Na^+/Na. However, the initial coulombic efficiency is rather low and only five cycles were shown.[159] Recently, Balaya and Jiao *et al.* also reported the Na storage properties of $Na_2Ti_3O_7$; however, the rate and cyclic performances are still unsatisfactory.[160,161] In addition, microspheric $Na_2Ti_3O_7$ consisting of tiny nanotubes was reported to show ultrafast charge–discharge rate and higher storage capacity in both crystalline and the surface of nanotubes.[162] The Na storage properties in $Na_2Ti_3O_7$ were investigated from thermodynamic and kinetic aspects to elaborate the unsatisfied performance.[163] Amorphous TiO_2 (Fig. 15a) nanotubes were also reported to show an initial reversible capacity of *ca.* 70 mA h g^{-1} and a capacity gradual increase in the subsequent 1–15 cycles in a voltage range of 0.9–2.5 V; however, further cycles were not shown.[164] Hu *et al.* initially demonstrated the interesting Na insertion into spinel $Li_4Ti_5O_{12}$ (Fig. 15b), which shows an average storage voltage of 0.91 V with a reversible capacity of 150 mA h g^{-1}. A new reversible three-phase reaction of $2Li_4Ti_5O_{12} + 6Na \leftrightarrow Li_7Ti_5O_{12} + Na_6LiTi_5O_{12}$ was proposed, which provided inspiration to consider Na storage mechanisms different from that of Li where a typical two-phase reaction is expected.[165] This result was further confirmed by a direct observation of the three-phase coexistence region through the advanced spherical aberration-corrected annular-bright-field (ABF) scanning transmission electron microscopy (STEM) technique (Fig. 16).[166] Furthermore, a sharp phase boundary of $Li_4Ti_5O_{12}/Li_7Ti_5O_{12}$ and $Li_7Ti_5O_{12}/Na_6LiTi_5O_{12}$ interfaces is clearly revealed at atomic scale. The sharp phase boundary between $Li_4Ti_5O_{12}$ and $Li_7Ti_5O_{12}$ can be understood because of the "zero-strain" characteristics of Li insertion in $Li_4Ti_5O_{12}$.[167] However, even the volume change between $Li_7Ti_5O_{12}$ and $Na_6LiTi_5O_{12}$ is quite large

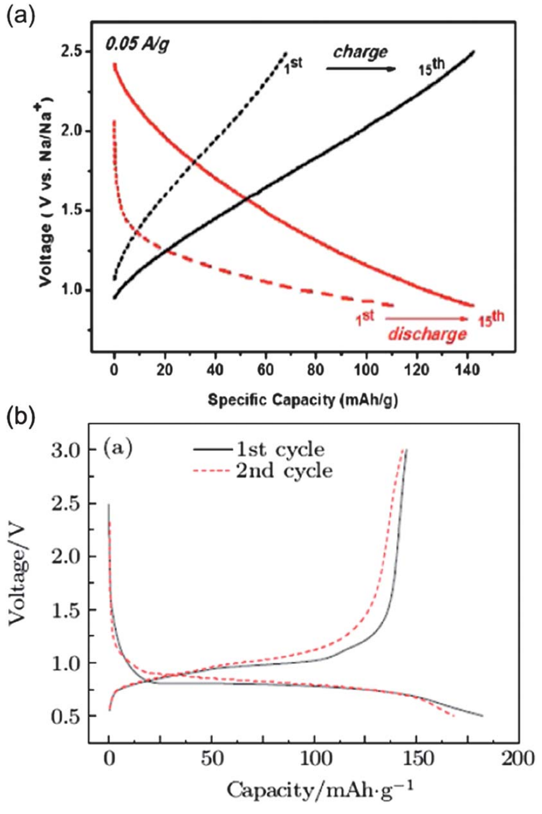

Fig. 15 The charge–discharge profiles of titanium-based oxides. (a) Amorphous TiO_2 nanotubes. (Reproduced with permission.[164] Copyright 2012, American Chemical Society.) (b) Spinel $Li_4Ti_5O_{12}$ (Reproduced with permission.[165] Copyright 2012, IOP-UK.).

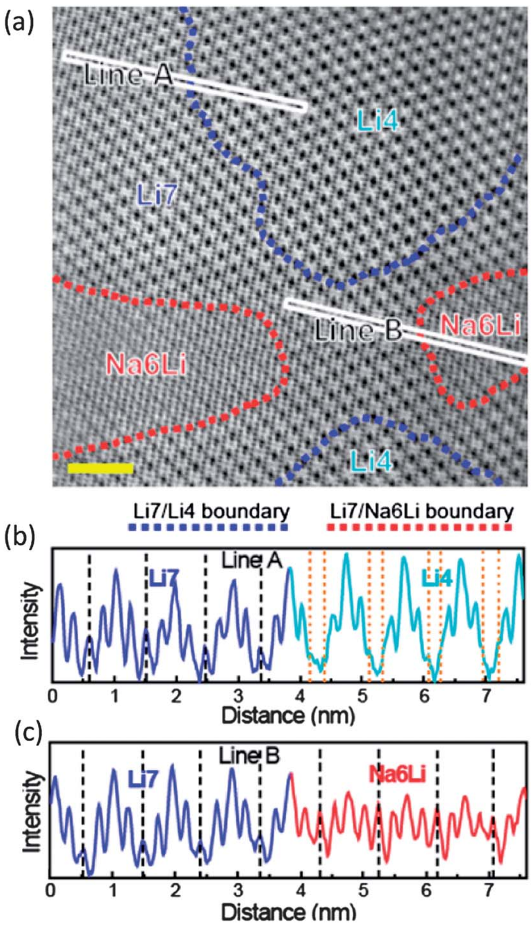

Fig. 16 (a) ABF-image of the co-existence of three-phase for the half electrochemically sodiated $Li_4Ti_5O_{12}$ nano-particles, (b) and (c) Line profiles crossing the $Li_7Ti_5O_{12}/Li_4Ti_5O_{12}$ (line A) and $Li_7Ti_5O_{12}/Na_6Li\ Ti_5O_{12}$ (line B) boundaries, respectively. (Reproduced with permission.[166] Copyright 2013, Nature Publishing Group.)

(13%),[166] a sharp phase boundary between them is still observed, suggesting that a sodium containing phase ($Na_6Li-Ti_5O_{12}$) could accommodate a large amount of strain.

Layered sulfides (*e.g.*, TiS_2, TaS_2 and MoS_2) were initially studied for Na storage with a Na insertion voltage of *ca.* 1.8–2 V.[14,18] Recently, sulfides, such as Ni_3S_2 (400 mA h g^{-1}, 0.84 V *vs.* Na^+/Na) and FeS_2 (447 mA h g^{-1}, 0–2.6 V), were also suggested as anodes for Na-ion batteries.[168,169] However, the cyclic stability of these sulfides need to be improved.

3.3 Alloy

A storage mechanism based on an alloy reaction was commonly investigated in Li-ion batteries because of the high storage capacity of such materials (*e.g.*, Si,[170] Sn,[171] *etc.*). In a Na system, a number of alloys have attracted interest. Komaba *et al.* reported that Sn electrodes exhibit a capacity of 500 mA h g^{-1} in a stoichiometric form of $Na_{15}Sn_4$ in a voltage range of 0–0.8 V,[172] which is consistent with the calculated results.[173] Nano-composites of Sb/C,[174] SnSb/C[175] and Sn/C,[176] exhibit a high capacity of 610 mA h g^{-1}, 544 mA h g^{-1} and 295 mA h g^{-1}, respectively, with good rate capability and cyclic stability (Fig. 17a). Amorphous phosphorus/C composites were recently reported to deliver the highest capacity of ~1800 mA h g^{-1} to date with an appropriate potential of 0.4 V *vs.* Na^+/Na and good cyclic performance.[177,178] On the other hand, the volume changes after Na insertion into these alloys are quite large (Fig. 17b),[173] however, it was interesting to find that cracking or fracture was not observed in the Sn particles in the initial cycles.[179] This behavior is very different from the case of Li storage in some alloys and deserves more fundamental studies. Nevertheless, practical applications of such materials with large volume change may suffer from the instability of the electrode, which is a common case in Li-ion batteries.[180]

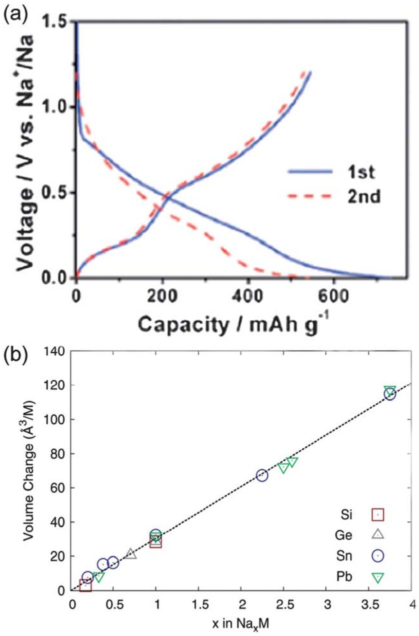

Fig. 17 (a) The charge–discharge profiles nano-composite SnSb/C (Reproduced with permission.[175] Copyright 2012, Royal Society of Chemistry.), (b) the volume change for known Na–M (M = Si, Ge, Sn, Pb *etc.*) increase linearly as function of Na content (Reproduced with permission.[173] Copyright 2011, The Electrochemical Society.).

3.4 Organic compounds

Most of the present organic anode materials with C=O bonds have been proposed to accommodate Li or Na *via* the reaction between alkali ions and C=O bonds. Dilithium terephthalate ($Li_2C_8H_4O_4$) originally proposed by Armand *et al.* can accommodate 2.3 Li per formula unit at about 0.8 V *vs.* Li^+/Li with good cyclic stability.[181] Recently, Hu *et al.* reported that the Na analogue of $Li_2C_8H_4O_4$, *i.e.* disodium terephthalate ($Na_2C_8H_4O_4$), can also deliver a reversible capacity of 250 mA h g^{-1} corresponding to a two-electron transfer at an average voltage of 0.45 V (Fig. 18).[182] However, the electronic conductivity of $Na_2C_8H_4O_4$ is rather poor; a large amount of carbon black is needed when preparing the electrode, thus leading to a low initial coulombic efficiency of *ca.* 60%, which mainly results from the side reaction between carbon black and the electrolyte. Hong and co-workers investigated various derivatives of disodium terephthalate with adjustable Na storage voltage.[183] They found that the thermodynamic and kinetic properties of organic electrodes can be controlled by introducing functional

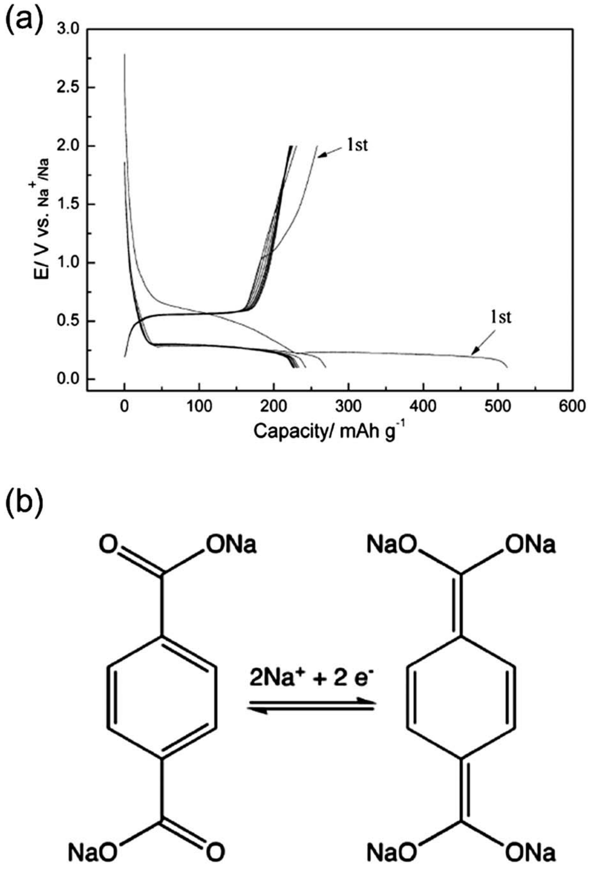

Fig. 18 (a) The charge–discharge curves of the $Na_2C_8H_4O_4$ electrode, (b) the scheme for Na storage mechanism in $Na_2C_8H_4O_4$. (Reproduced with permission.[182] Copyright 2012, Wiley-VCH.)

groups to the benzene–carboxylate. Amine and co-workers also examined a series of organic carboxylate based materials, and assembled a 3.6 V full cell using $Na_2C_8H_4O_4$ anode and $Na_{0.75}Mn_{0.7}Ni_{0.23}O_2$ cathode, which exhibits a capacity above 268 mA h g^{-1} (anode-limited capacity) after 50 cycles.[184] Chihara and co-workers recently reported that bulk $Na_2C_6O_6$/C composite delivers a high reversible capacity of 270 mA h g^{-1} in a voltage range of 1–2.9 V *vs.* Na^+/Na in the first cycle. However, the coulombic efficiency and cyclic stability still need to be improved.[185] Organic electrode materials with high storage capacity, low cost and facile synthesis can be largely used as the next-generation electrode material if the electronic conductivity issue can be solved.

4 Electrolytes

4.1 Organic liquid electrolytes

Electrolyte, an indispensable part of batteries, offers alkali ion conduction and transport media between the cathode and anode, which refers to the electrochemical properties and the safety issues of a battery.[186–189] Optimizing the electrolyte is important for the actual application of Na-ion batteries. Various organic liquid electrolytes have been investigated by several groups. Palacín's group recently evaluated three kinds of salt ($NaClO_4$, NaTFSI, $NaPF_6$) combined with different solvents (PC, EC, DMC, DME, DEC, THF, triglyme and their mixtures) by testing their thermal stability, conductivity, viscosity and electrochemical window.[190] They found that the $NaClO_4$ or $NaPF_6$ in the EC : PC solvent mixture is the best electrolyte for the hard carbon anode.[190] Hu *et al.* first proposed the use of a new salt of NaFSI dissolved in organic PC solvent. (Note that with such excellent properties as low melting point (224.2 K), high boiling point (514.9 K), high flash point (405.2 K), high dielectric constant, high chemical stability, and wide electrochemical window, PC is an attractive candidate solvent for non-aqueous electrolytes for batteries operated at both high and low temperatures.[186–188]) NAFSI-based electrolytes can significantly improve the storage performance of both $Na_3V_2(PO_4)_3$/C cathode and $Na_2C_8H_4O_4$ anode.[98,182] NaFSA-C1C3pyrFSA ionic liquid was reported as a new electrolyte with a high electrochemical oxidation window up to 5.2 V at 353 K and a conductivity of 15.6 mS cm^{-1}.[191] Aside from the intrinsic parameters of the electrolyte, the controllable surface reaction (SEI reaction) between the electrolyte and the electrode material is also important for a good electrolyte system. Fluoroethylene carbonate was recently reported as an effective functional additive for modifying the SEI layer and improving the reversibility of electrochemical Na insertion for both hard carbon and $NaNi_{0.5}Mn_{0.5}O_2$ electrodes in non-aqueous Na batteries.[192]

4.2 Solid state electrolytes

Solid state electrolyte can potentially avoid the safety issue resulting from the use of organic liquid electrolytes, such as leakage and flammability. This step is important in realizing all-solid-state energy storage devices; thereby it has been attracting significant attention for a long time. β-Al_2O_3 ($Na_2O\cdot 11Al_2O_3$) or β''-Al_2O_3 is an excellent fast Na^+ ionic conductor with a layered structure and a two-dimensional (2-D) Na^+ ion migration, which has been widely used as a solid electrolyte in high-temperature Na–S batteries.[193] Another interesting and attractive Na^+ ionic conductor is based on crystalline NASICON compounds of $Na_{1+x}Zr_3P_{3-x}Si_xO_{12}$ ($0 \le x \le 3$), which was first proposed by Hong and Goodenough.[91,92] These NASICON electrolytes were demonstrated to have a high Na^+ ionic conductivity of 6×10^{-4} S cm^{-1} at room temperature.[194] Recently, Hayashi and co-workers reported a super ionic glass-ceramic Na_3PS_4 ($\sim 10^{-4}$ S cm^{-1}) as the electrolyte in an all-solid-state battery operated at room temperature.[195] All-solid-state batteries with high safety qualifications must be developed as the next-generation battery for the realization of a low-carbon society in the near future.

5 Some new perspectives in Na-ion batteries

5.1 Aqueous Na-ion batteries

Using an aqueous electrolyte in a rocking-chair battery is an attractive approach to avoid the high cost and low safety issues resulting from organic liquid electrolytes. Many aqueous Li-ion batteries, such as $VO_2/LiMn_2O_4$, $LiV_3O_8/LiNi_{0.81}Co_{0.19}O_2$, $LiV_3O_8/LiCoO_2$ and $LiTi_2(PO_4)_3/LiMn_2O_4$ systems have been reported (Fig. 19a).[22–27] However, practical applications of aqueous Li-ion battery are not likely because of the limited Li resources. In contrast, developing aqueous Na-ion batteries is more meaningful and practical because of the huge abundance of Na resources (NaCl, Na_2SO_4, $NaNO_3$, *etc.*). A $Na_{0.44}MnO_2$/activated carbon full cell recently demonstrated in an aqueous electrolyte delivers high rate capability (Fig. 19b) with an excellent cycle life over 1000 cycles at 4 C.[28] However, the energy density of the $Na_{0.44}MnO_2$/activated carbon system is too low for practical applications. Chiang's group reported a high energy density aqueous $Na_{0.44}MnO_2/NaTi_2(PO_4)_3$ system (Fig. 19c), which could exhibit a theoretical energy density of ~33 W h kg^{-1}, as estimated from only the mass of cathode and anode.[29] Cui's group first demonstrated that hexacyanoferrate electrodes can reversibly store alkali ions in aqueous electrolytes.[129–131] A high-rate and long cycle life (1000 cycles) aqueous battery was constructed based on a copper hexacyanoferrate cathode and a activated carbon/polypyrrole hybrid anode.[131] Recently, an aqueous rechargeable battery with $Na_2NiFe(CN)_6$ and $NaTi_2(PO_4)$ as cathode and anode respectively, represent good rate and cycle life with a theoretical energy density of 42.5 W h kg^{-1}.[196] Thus, reaching an even higher energy density by choosing the proper electrode materials is possible. Nevertheless, an aqueous electrolyte system is more complicated than an organic system because of the (1) elimination of residual O_2 in the electrolyte, (2) protection of the electrode stability in an aqueous electrolyte, (3) inhibition of H_3O^+ co-intercalation into the electrode and (4) efficient internal consumption of O_2 and H_2 produced from cathode and anode sides when overcharged or overdischarged or improperly operated in a close aqueous battery system. All these issues are important for the practical application of an aqueous battery system.[23,27]

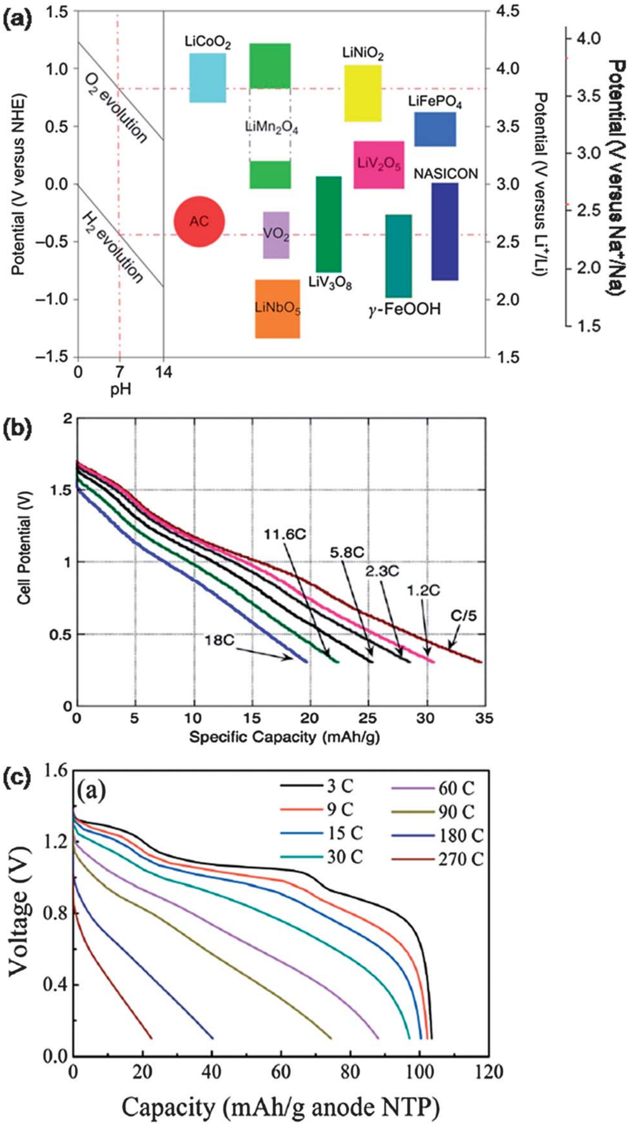

Fig. 19 (a) The intercalation potential of some electrode materials that could be employed for aqueous Li-/Na-ion batteries (Reproduced with permission.[23] Copyright 2012, Nature Publishing Group.). The rate performance of aqueous full cells: (b) $Na_{0.44}MnO_2$/active carbon (Reproduced with permission.[28] Copyright 2010, Elsevier.) and (c) $NaTi_2(PO_4)_3/Na_{0.44}MnO_2$. (Reproduced with permission.[29] Copyright 2012, Wiley-VCH.)

5.2 High throughput *ab initio* calculations

Searching for new electrode materials experimentally, including synthesis and electrochemical testing of a new material, is relatively time consuming. Recently, Ceder's group proposed a new approach based on high throughput density functional theory (DFT) computation to search for new promising electrode materials. This approach starts with existing compounds in the Inorganic Crystal Structure Database (ICSD), and it could be helpful in exploring new electrode materials more efficiently by identifying and focusing on the most promising chemistries. This group has performed a computational search and has identified an entirely new mixed polyanionic $Li_3Mn(CO_3)(PO_4)$ as a Li-ion battery cathode. They also calculated a series of Na based mixed polyanionic compounds. Many Na-based phases (*e.g.*, $Na_xM(YO_3)(XO_4)$; M = a redox active metal; Y = C, B; X = Si, P, As, and $x = 0$ to 3) have been predicted to be thermodynamically stable in the sidorekite structure, with a small volume change after Na extraction. This high throughput *ab initio* calculation approach can also be employed to analyze and evaluate the capacity, voltage, specific energy, energy density, and thermal stability of a series of new compounds with specified structure.[20,21]

6 Reversible energy storage and transport mechanism in Na-ion batteries

Possible Li storage mechanisms have been summarized in a previous review.[9] Similar energy storage mechanisms are also evidenced in Na-ion batteries as listed in Table 2. Layered Na_xMO_2 (M = Co, Mn, V, *etc.*) includes both intercalation and phase transition reactions during the Na insertion/extraction process. Na_xMO_2 usually includes various complex single- and two-phase regions during the Na insertion–extraction process.[31,33,66] While Na reversible storage in $Na_3V_2(PO_4)_3$ corresponds to a typical two-phase reaction.[98] Spinel $Li_4Ti_5O_{12}$ represents a novel three-phase separation reaction during Na insertion caused by the different size of Na^+ and Li^+ ions.[165,166] Oxides or sulfides, such as $NiCo_2O_4$ and FeS_2, exhibit a reversible conversion reaction between Na oxide/sulfide and the transition metal.[153,169] Alloy composites, such as SnSb/C, store Na *via* an alloying reaction.[175] The energy storage in the organic electrode is commonly associated with chemical bonding (*e.g.*, $Na_2C_8H_4O_4$ (ref. 182)) or free radical doping/dedoping mechanism (aniline–nitroaniline copolymer[139]). The amorphous TiO_2 stores Na through a surface charging.[164] Furthermore, new energy storage mechanisms may be proposed with the continuous investigation in Na-ion batteries. As a matter of fact, a similar energy storage mechanism in Li- and Na-ion batteries enables us to understand and design new electrode materials for Na-ion batteries based on experience gained from Li-ion batteries. Meanwhile, the difference between alkali ion storage in Na/Li analogues also allows us to further understand the structure and storage mechanism of electrode materials.

In addition, the understanding of sodium transport properties is very important in designing new electrode materials with specific structures. However, only a few publications elaborate the sodium transport properties of electrode materials so far. Since the radius of a Na^+ ion is much larger than that of a Li^+ ion, it was once generally believed that the transport of Na^+ ions is sluggish in Na storage electrodes. In fact the sodium transport properties are greatly related to the crystal structures. Ceder and co-workers showed that the Na^+ ion migration barrier can be lower than that of Li^+ ion in the layered structure.[197] Our group investigated the Na^+ ion transport properties in layered $Na_2Ti_3O_7$ with the assistance of DFT calculation. It was found that the Na^+ ion transport along the TiO_6 layer has a rather low activation energy of 0.186 meV, forming a quasi-3D trajectory on the basis of a vacancy-hopping mechanism.[163] In addition, due to the larger size of Na^+ ion, the Na storage in spinel is rarely reported. We first reported detailed

Table 2 The energy storage mechanism in Na-ion batteries

Storage mechanism	Examples
Intercalation	P2-$Na_{1.0}Li_{0.2}Ni_{0.25}Mn_{0.75}O_y$.[64] *etc.*
Phase transition	$Na_3V_2(PO_4)_3$,[98] Na_2FePO_4F,[116] $Li_4Ti_5O_{12}$,[165] *etc.*
Conversion	$NiCo_2O_4$,[153] FeS_2,[169] *etc.*
Alloying	Sn/C, Sb/C, SnSb/C,[175] *etc.*
Reversible chemical bonding	$Na_2C_8H_4O_4$,[182] *etc.*
Doping and dedoping	Aniline–nitroaniline copolymer[139]
Surface or interface charging	Amorphous TiO_2 [164]
Under potential deposition	……

studies on the Na^+ ion storage and transport mechanism in spinel $Li_4Ti_5O_{12}$ with DFT calculations.[165,166] We showed that the Na^+ ion transport kinetics is much poorer than that of Li^+ ion. The calculated activation energy for Na^+ ion transport is as high as 0.9 eV, indicating the sluggish Na^+ ion diffusion in such a cubic close-packed structure. More detailed perspectives and investigation are expected to elaborate the transport mechanism in Na-ion batteries.

7 Personal outlook

Room-temperature Na-ion batteries have attracted a great deal of attention in recent years; however, due to the high energy density of Li-ion batteries, the potential markets for these batteries could be used for the devices in which cycle life and cost are more essential factors than energy density, such as in large-scale electricity storage for renewable forms of energies and smart grids. To date, a large number of compounds have been proposed as electrode materials for Na-ion batteries as reviewed in the present work. Searching for new electrode materials for Na-ion batteries with high energy and power density, but with low volume change (or low-strain) during cycling (This point is critically important for realizing a very long cyclic performance.), remains a great challenge, particularly for anodes. The high throughput *ab initio* calculation approach may facilitate research on new electrode materials in the near future. Overall, common experiences from Li-ion batteries could be considered when designing and understanding an electrode material for Na-ion batteries. The different storage behaviors, such as in $NaCrO_2/LiCrO_2$ and $NaMnO_2/LiMnO_2$, are important fundamental scientific questions in understanding the influence of the structure on electrochemical performance. Furthermore, one might worry about the Na^+ ion diffusion kinetics might be a problem because of its larger ionic size compared with Li^+ ion. However, actually, the time for discovering Na^+ ion fast ionic conductors is even earlier than Li^+ ones. A famous fast Na^+ ionic conductor is β''-Al_2O_3 which was identified almost 50 years ago.[193] The other interesting one is $Na_{1+x}Zr_3P_{3-x}Si_xO_{12}$ $(0 \le x \le 3)$ based on an open NASICON structure with suitable size of Na^+ ion transport channel.[91,92] A recent DFT calculation shows that the activation energy of Na^+ ion diffusion in layered compounds (*e.g.*, $ACoO_2$) is even lower than that of Li^+ ion diffusion.[197] Therefore, Na^+ ion diffusion will be not a problem if a proper structure is selected.

Fig. 20 shows the transition metal redox potential in a Na-ion battery *vs.* a Li-ion battery, where it can be seen that the Na compounds exhibit a relatively lower voltage of 0.3–1.2 V. In addition, most of the present cathodes are referred to oxides, especially the layered Na_xMO_2. Although layered oxides generally exhibit higher storage capacity, it is still a tough work to elaborate and enhance the structure and thermal stability of layered compounds for their applications, particularly for stationary batteries. The composition and arrangement modification of the TM layer may enhance the structure stability of layered oxides compounds by introducing inactive element into the TM layer, such as Li^+, Mg^{2+}, Al^{3+}, Mn^{4+}, *etc.* Alternatively, Na transition metal phosphates offer higher structural and thermal stability, as well as higher storage voltage, which would be attractive candidates after kinetics optimization.

Moreover, the storage voltage and electrochemical performance of electrode materials are strongly related to their crystalline structures. The crystalline structures of several available cathode materials, including both oxides and phosphates, are shown in Fig. 21. Such information can provide insightful guidelines in designing new electrode materials for Na-ion batteries.

Specific capacities *vs.* voltage for the currently proposed electrode material are displayed in Fig. 22, which provides a full picture of recent potential electrode materials. Most cathodes, including TM redox, deliver a relatively lower capacity than their Li analogues. Thus, storage capacity can still be greatly improved. For anodes, alloy compounds exhibit higher capacity; however, the resulting large volume change during Na insertion–extraction is not suitable for a long-term stability as demonstrated in Li-ion batteries. Thus, developing zero- or low-strain electrode materials from the viewpoint of long-life stationary batteries is necessary. (Note that this is quite challenging particularly for sodium based electrodes because of the larger ionic size of Na^+ ion compared with Li^+ ion.) Carbon-based materials are mostly investigated, exhibiting possible practical applications in Na-ion batteries. However, the Na storage voltage in hard carbon is relatively low and near zero *vs.* Na^+/Na, thus resulting in Na metal deposition on its surface during an improper operation or fast charging, and giving rise to major safety concerns. Aside from carbon, sodium titanate oxides with small volume change are also attractive. In addition, organic compounds with low cost and high storage capacity have also emerged as a new promising direction for future battery technology.

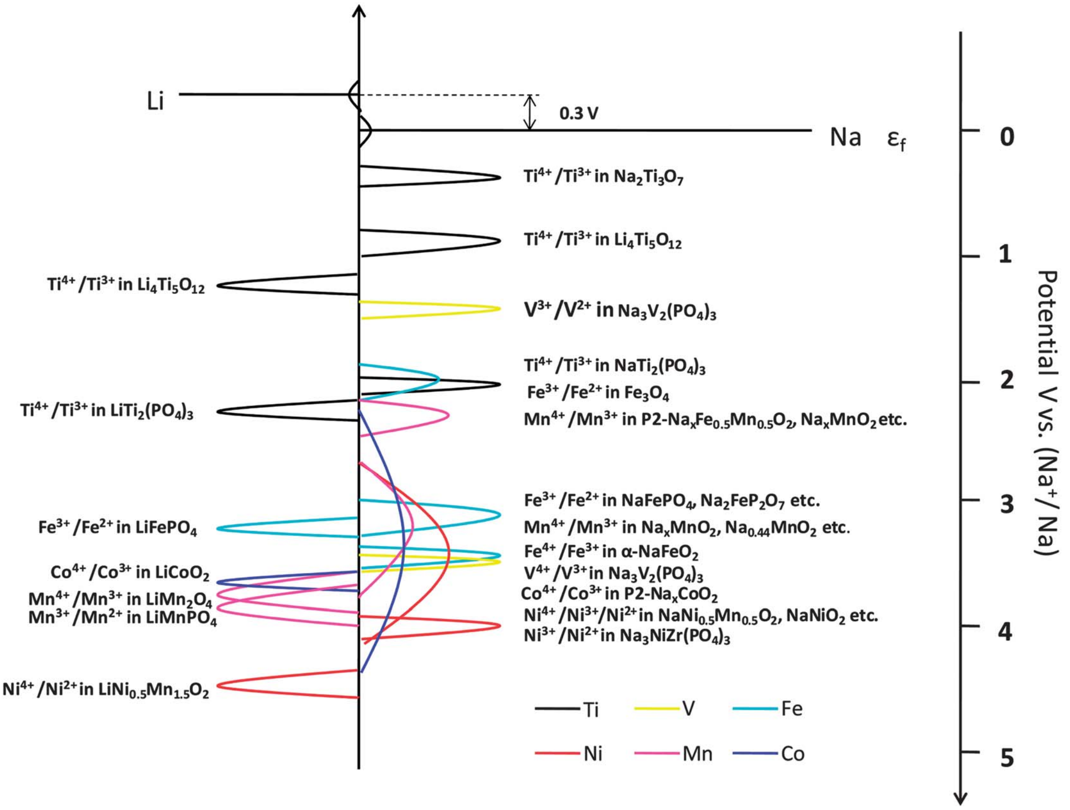

Fig. 20 The electrode potential for transition metal redox couples.

Furthermore, the calculated energy density *vs.* average operation voltage of full cells combined oxide/phosphate cathodes with the hard carbon anode is illustrated in Fig. 23. (Note that the capacities and average storage voltage of the electrodes are referred to ref. 12, 57, 61, 64, 67, 78, 90, 98 and 116) It can be seen that a Na-ion full cell could provide a theoretical energy

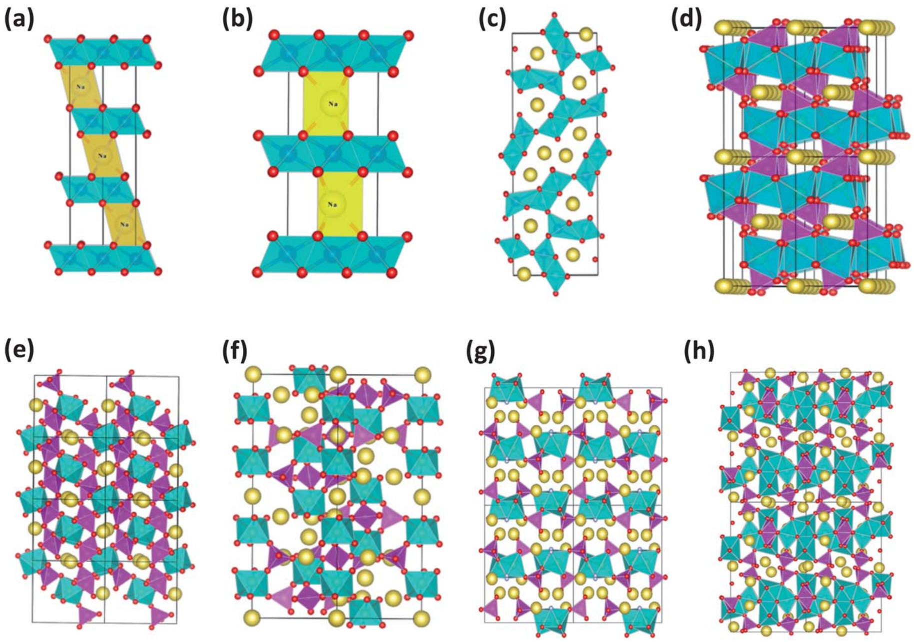

Fig. 21 The crystalline structure of several available cathode materials for Na-ion batteries. (a) O3-$NaMO_2$, (b) P2-Na_xMO_2, (c) $Na_{0.44}MnO_2$, (d) olivine $NaFePO_4$, (e) $Na_2FeP_2O_7$, (f) NASICON-$Na_3V_2(PO_4)_3$, (g) Na_2FePO_4F, (h) $Na_4Fe_3(PO_4)_2P_2O_7$.

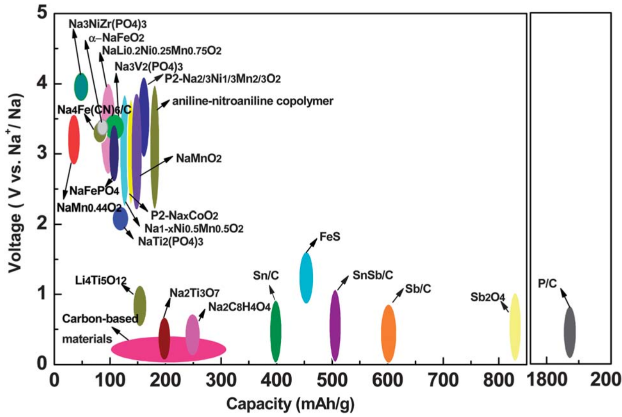

Fig. 22 The relationship between capacity and voltage for present electrode materials in Na-ion batteries.

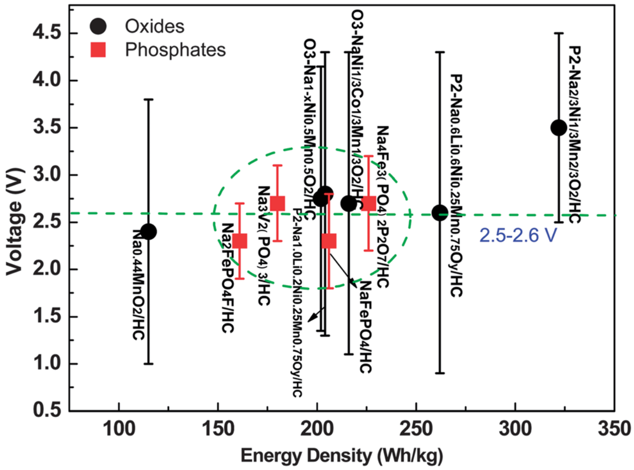

Fig. 23 The energy density and average operation voltage of full cells combined oxide/phosphate cathodes with hard carbon as anodes.

density of *ca.* 200 W h kg^{-1} with an average operation voltage between 2.5 V and 2.6 V, demonstrating that a Na-ion based battery technology would provide an acceptable energy density if proper cathode and anode materials are selected. Even though these values are lower than those of Li-ion batteries, they are still higher than those of commonly used lead-acid secondary batteries which have serious environmental problems. The successful development of room-temperature Na-ion batteries would provide a great opportunity to replace lead-acid batteries in some applications.

Finally, searching for a new electrolyte system is another important aspect for the application of Na-ion batteries in ESS. Unlike Li-ion batteries, graphite cannot be used as an anode for Na-ion batteries; thus, a variety of other cheaper Na salts and solvents can be chosen, besides PF_6^- based salt and carbonate solvents commonly used in Li-ion batteries. Moreover, developing low cost and high safety aqueous Na-ion batteries is also a meaningful endeavor. We believe that low-cost, long-life and room-temperature Na-ion batteries will be promising for applications in large-scale ESS in the future.

Acknowledgements

This work was supported by funding from the "863" Project (2009AA033101), NSFC (51222210, 11234013), CAS project (KJCX2-YW-W26) and One Hundred Talent Project of the Chinese Academy of Sciences.

References

1 B. Dunn, H. Kamath and J. M. Tarascon, *Science*, 2011, **334**, 928–935.
2 Z. G. Yang, J. L. Zhang, M. C. W. Kintner-Meyer, X. C. Lu, D. W. Choi, J. P. Lemmon and J. Liu, *Chem. Rev.*, 2011, **111**, 3577–3613.
3 H. Ibrahim, A. Ilinca and J. Perron, *Renew. Sust. Energy Rev.*, 2008, **12**, 1221–1250.
4 H. Chen, T. N. Cong, W. Yang, C. Tan, Y. Li and Y. Ding, *Prog. Nat. Sci.*, 2009, **19**, 291–312.
5 X. C. Lu, G. G. Xia, J. P. Lemmon and Z. G. Yang, *J. Power Sources*, 2010, **195**, 2431–2442.
6 L. Joerissen, J. Garche, C. Fabjan and G. Tomazic, *J. Power Sources*, 2004, **127**, 98–104.
7 http://en.wikipedia.org/wiki/File:Elemental_abundances.svg.
8 C.-X. Zu and H. Li, *Energy Environ. Sci.*, 2011, **4**, 2614–2624.
9 V. Palomares, P. Serras, I. Villaluenga, K. B. Hueso, J. Carretero-Gonzalez and T. Rojo, *Energy Environ. Sci.*, 2012, **5**, 5884–5901.
10 B. L. Ellis and L. F. Nazar, *Curr. Opin. Solid State Mater. Sci.*, 2012, **16**, 168–177.
11 S. W. Kim, D. H. Seo, X. H. Ma, G. Ceder and K. Kang, *Adv. Energy Mater.*, 2012, **2**, 710–721.
12 M. D. Slater, D. Kim, E. Lee and C. S. Johnson, *Adv. Funct. Mater.*, 2013, **23**, 947–958.
13 K. Mizushima, P. C. Jones, P. J. Wiseman and J. B. Goodenough, *Mater. Res. Bull.*, 1980, **15**, 783–789.
14 A. S. Nagelberg and W. L. Worrell, *J. Solid State Chem.*, 1979, **29**, 345–354.
15 J. P. Parant, R. Olazcuag, M. Devalett, C. Fouassie and P. Hagenmul, *J. Solid State Chem.*, 1971, **3**, 1–5.
16 C. Delmas, C. Fouassier and P. Hagenmuller, *Physica B+C*, 1980, **99**, 81–85.
17 J. J. Braconnier, C. Delmas, C. Fouassier and P. Hagenmuller, *Mater. Res. Bull.*, 1980, **15**, 1797–1804.
18 M. S. Whittingham, *Prog. Solid State Chem.*, 1978, **12**, 41–99.
19 K. B. Hueso, M. Armand and T. Rojo, *Energy Environ. Sci.*, 2013, **6**, 734–749.
20 G. Hautier, A. Jain, H. L. Chen, C. Moore, S. P. Ong and G. Ceder, *J. Mater. Chem.*, 2011, **21**, 17147–17153.
21 G. Hautier, A. Jain, S. P. Ong, B. Kang, C. Moore, R. Doe and G. Ceder, *Chem. Mater.*, 2011, **23**, 3495–3508.
22 W. Li, J. R. Dahn and D. S. Wainwright, *Science*, 1994, **264**, 1115–1118.
23 J. Y. Luo, W. J. Cui, P. He and Y. Y. Xia, *Nat. Chem.*, 2010, **2**, 760–765.
24 J. Kohler, H. Makihara, H. Uegaito, H. Inoue and M. Toki, *Electrochim. Acta*, 2000, **46**, 59–65.

25 C. Z. Wu, Z. P. Hu, W. Wang, M. A. Zhang, J. L. Yang and Y. Xie, *Chem. Commun.*, 2008, 3891–3893.

26 H. Yadegari, A. Jabbari and H. Heli, *J. Solid State Electrochem.*, 2012, **16**, 227–234.

27 Y. Wang, J. Yi and Y. Xia, *Adv. Energy Mater.*, 2012, **2**, 830–840.

28 J. F. Whitacre, A. Tevar and S. Sharma, *Electrochem. Commun.*, 2010, **12**, 463–466.

29 Z. Li, D. Young, K. Xiang, W. C. Carter and Y.-M. Chiang, *Adv. Energy Mater.*, 2012, **3**, 290–294.

30 C. Delmas, J. J. Braconnier, C. Fouassier and P. Hagenmuller, *Solid State Ionics*, 1981, **3–4**, 165–169.

31 A. Mendiboure, C. Delmas and P. Hagenmuller, *J. Solid State Chem.*, 1985, **57**, 323–331.

32 M. M. Doeff, M. Y. Peng, Y. P. Ma and L. C. Dejonghe, *J. Electrochem. Soc.*, 1994, **141**, L145–L147.

33 R. Berthelot, D. Carlier and C. Delmas, *Nat. Mater.*, 2011, **10**, U74.

34 J. Molenda, C. Delmas and P. Hagenmuller, *Solid State Ionics*, 1983, **9–10**, 431–435.

35 L. W. Shacklette, T. R. Jow and L. Townsend, *J. Electrochem. Soc.*, 1988, **135**, 2669–2674.

36 A. Caballero, L. Hernan, J. Morales, L. Sanchez, J. S. Pena and M. A. G. Aranda, *J. Mater. Chem.*, 2002, **12**, 1142–1147.

37 X. H. Ma, H. L. Chen and G. Ceder, *J. Electrochem. Soc.*, 2011, **158**, A1307–A1312.

38 J. Reed, G. Ceder and A. Van der Ven, *Electrochem. Solid-State Lett.*, 2001, **4**, A78–A81.

39 Y. Shao-Horn, S. A. Hackney, A. R. Armstrong, P. G. Bruce, R. Gitzendanner, C. S. Johnson and M. M. Thackeray, *J. Electrochem. Soc.*, 1999, **146**, 2404–2412.

40 A. Yamada, M. Tanaka, K. Tanaka and K. Sekai, *J. Power Sources*, 1999, **81**, 73–78.

41 M. Dolle, S. Patoux and M. M. Doeff, *Chem. Mater.*, 2005, **17**, 1036–1043.

42 S. Patoux, M. Dolle and M. M. Doeff, *Chem. Mater.*, 2005, **17**, 1044–1054.

43 Y. Takeda, K. Nakahara, M. Nishijima, N. Imanishi, O. Yamamoto, M. Takano and R. Kanno, *Mater. Res. Bull.*, 1994, **29**, 659–666.

44 N. Yabuuchi, H. Yoshida and S. Komaba, *Electrochemistry*, 2012, **80**, 716–719.

45 J. Zhao, L. Zhao, N. Dimov, S. Okada and T. Nishida, *J. Electrochem. Soc.*, 2013, **160**, A3077–A3081.

46 N. Yabuuchi, M. Kajiyama, J. Iwatate, H. Nishikawa, S. Hitomi, R. Okuyama, R. Usui, Y. Yamada and S. Komaba, *Nat. Mater.*, 2012, **11**, 512–517.

47 J. S. Thorne, R. A. Dunlap and M. N. Obrovac, *J. Electrochem. Soc.*, 2013, **160**, A361–A367.

48 S. Komaba, T. Nakayama, A. Ogata, T. Shimizu, C. Takei, S. Takada, A. Hokura and I. Nakai, *ECS Trans.*, 2009, **16**, 43–55.

49 S. Komaba, C. Takei, T. Nakayama, A. Ogata and N. Yabuuchi, *Electrochem. Commun.*, 2010, **12**, 355–358.

50 J. J. Ding, Y. N. Zhou, Q. Sun and Z. W. Fu, *Electrochem. Commun.*, 2012, **22**, 85–88.

51 C.-Y. Chen, K. Matsumoto, T. Nohira, R. Hagiwara, A. Fukunaga, S. Sakai, K. Nitta and S. Inazawa, *J. Power Sources*, 2013, **237**, 52–57.

52 S.-T. Myung, S. Komaba, N. Hirosaki, N. Kumagai, K. Arai, R. Kodama and I. Nakai, *J. Electrochem. Soc.*, 2003, **150**, A1560–A1568.

53 S. Miyazaki, S. Kikkawa and M. Koizumi, *Synth. Met.*, 1983, **6**, 211–217.

54 J. Molenda and A. Stoklosa, *Solid State Ionics*, 1990, **38**, 1–4.

55 P. Vassilaras, X. H. Ma, X. Li and G. Ceder, *J. Electrochem. Soc.*, 2013, **160**, A207–A211.

56 S. Komaba, N. Yabuuchi, T. Nakayama, A. Ogata, T. Ishikawa and I. Nakai, *Inorg. Chem.*, 2012, **51**, 6211–6220.

57 M. Sathiya, K. Hemalatha, K. Ramesha, J. M. Tarascon and A. S. Prakash, *Chem. Mater.*, 2012, **24**, 1846–1853.

58 D. Kim, E. Lee, M. Slater, W. Q. Lu, S. Rood and C. S. Johnson, *Electrochem. Commun.*, 2012, **18**, 66–69.

59 S. Okada, Y. Takahashi, T. Kiyabu, T. Doi, J.-I. Yamaki and T. Nishida, *Meet. Abstr.*, 2006, **MA2006–02**, 201.

60 D. Carlier, J. H. Cheng, R. Berthelot, M. Guignard, M. Yoncheva, R. Stoyanova, B. J. Hwang and C. Delmas, *Dalton Trans.*, 2011, **40**, 9306–9312.

61 Z. H. Lu and J. R. Dahn, *J. Electrochem. Soc.*, 2001, **148**, A1225–A1229.

62 D. Buchholz, A. Moretti, R. Kloepsch, S. Nowak, V. Siozios, M. Winter and S. Passerini, *Chem. Mater.*, 2013, **25**, 142–148.

63 D. D. Yuan, W. He, F. Pei, F. Y. Wu, Y. Wu, J. F. Qian, Y. L. Cao, X. P. Ai and H. X. Yang, *J. Mater. Chem. A*, 2013, **1**, 3895–3899.

64 D. Kim, S. H. Kang, M. Slater, S. Rood, J. T. Vaughey, N. Karan, M. Balasubramanian and C. S. Johnson, *Adv. Energy Mater.*, 2011, **1**, 333–336.

65 H. M. Liu, H. S. Zhou, L. P. Chen, Z. F. Tang and W. S. Yang, *J. Power Sources*, 2011, **196**, 814–819.

66 D. Hamani, M. Ati, J. M. Tarascon and P. Rozier, *Electrochem. Commun.*, 2011, **13**, 938–941.

67 F. Sauvage, L. Laffont, J. M. Tarascon and E. Baudrin, *Inorg. Chem.*, 2007, **46**, 3289–3294.

68 Y. L. Cao, L. F. Xiao, W. Wang, D. W. Choi, Z. M. Nie, J. G. Yu, L. V. Saraf, Z. G. Yang and J. Liu, *Adv. Mater.*, 2011, **23**, 3155–3160.

69 E. Hosono, T. Saito, J. Hoshino, M. Okubo, Y. Saito, D. Nishio-Hamane, T. Kudo and H. S. Zhou, *J. Power Sources*, 2012, **217**, 43–46.

70 H. Kim, D. J. Kim, D. H. Seo, M. S. Yeom, K. Kang, D. K. Kim and Y. Jung, *Chem. Mater.*, 2012, **24**, 1205–1211.

71 A. Kuhn, N. Menendez, F. GarciaAlvarado, E. Moran, J. D. Tornero and M. A. AlarioFranco, *J. Solid State Chem.*, 1997, **130**, 184–191.

72 A. K. Padhi, K. S. Nanjundaswamy and J. B. Goodenough, *J. Electrochem. Soc.*, 1997, **144**, 1188–1194.

73 A. K. Padhi, K. S. Nanjundaswamy, C. Masquelier, S. Okada and J. B. Goodenough, *J. Electrochem. Soc.*, 1997, **144**, 1609–1613.

74 J. N. Bridson, S. E. Quinlan and P. R. Tremaine, *Chem. Mater.*, 1998, **10**, 763–768.

75 R. Hammond and J. Barbier, *Acta Crystallogr., Sect. B: Struct. Sci.*, 1996, **52**, 440–449.

76 K. Zaghib, J. Trottier, P. Hovington, F. Brochu, A. Guerfi, A. Mauger and C. M. Julien, *J. Power Sources*, 2011, **196**, 9612–9617.

77 J. Moring and E. Kostiner, *J. Solid State Chem.*, 1986, **61**, 379–383.

78 P. Moreau, D. Guyomard, J. Gaubicher and F. Boucher, *Chem. Mater.*, 2010, **22**, 4126–4128.

79 T. Shiratsuchi, S. Okada, J. Yamaki and T. Nishida, *J. Power Sources*, 2006, **159**, 268–271.

80 J. M. Zhao, Z. L. Jian, J. Ma, F. C. Wang, Y. S. Hu, W. Chen, L. Q. Chen, H. Z. Liu and S. Dai, *ChemSusChem*, 2012, **5**, 1495–1500.

81 Y. L. Liu, Y. H. Xu, X. G. Han, C. Pellegrinelli, Y. J. Zhu, H. L. Zhu, J. Y. Wan, A. C. Chung, O. Vaaland, C. S. Wang and L. B. Hu, *Nano Lett.*, 2012, **12**, 5664–5668.

82 K. T. Lee, T. N. Ramesh, F. Nan, G. Botton and L. F. Nazar, *Chem. Mater.*, 2011, **23**, 3593–3600.

83 S. P. Ong, V. L. Chevrier and G. Ceder, *Phys. Rev. B: Condens. Matter Mater. Phys.*, 2011, **83**, 075112–075118.

84 P. Barpanda, T. Ye, S. Nishimura, S. C. Chung, Y. Yamada, M. Okubo, H. S. Zhou and A. Yamada, *Electrochem. Commun.*, 2012, **24**, 116–119.

85 T. Honma, T. Togashi, N. Ito and T. Komatsu, *J. Ceram. Soc. Jpn.*, 2012, **120**, 344–346.

86 H. Kim, R. A. Shakoor, C. Park, S. Y. Lim, J.-S. Kim, Y. N. Jo, W. Cho, K. Miyasaka, R. Kahraman, Y. Jung and J. W. Choi, *Adv. Funct. Mater.*, 2013, **23**, 1147–1155.

87 P. Barpanda, J. Lu, T. Ye, M. Kajiyama, S.-C. Chung, N. Yabuuchi, S. Komaba and A. Yamada, *RSC Adv.*, 2013, **3**, 3857–3860.

88 P. Barpanda, T. Ye, M. Avdeev, S.-C. Chung and A. Yamada, *J. Mater. Chem. A*, 2013, **1**, 4194–4197.

89 F. Sanz, C. Parada, J. M. Rojo and C. Ruiz-Valero, *Chem. Mater.*, 2001, **13**, 1334–1340.

90 H. Kim, I. Park, D. H. Seo, S. Lee, S. W. Kim, W. J. Kwon, Y. U. Park, C. S. Kim, S. Jeon and K. Kang, *J. Am. Chem. Soc.*, 2012, **134**, 10369–10372.

91 H. Y. P. Hong, *Mater. Res. Bull.*, 1976, **11**, 173–182.

92 J. B. Goodenough, H. Y. P. Hong and J. A. Kafalas, *Mater. Res. Bull.*, 1976, **11**, 203–220.

93 A. K. Padhi, K. S. Nanjundaswamy, C. Masquelier and J. B. Goodenough, *J. Electrochem. Soc.*, 1997, **144**, 2581–2586.

94 D. B. Porter, R. Olazcuaga, C. Delmas, F. Cherkaoui, R. Brochu and G. Leflem, *Rev. Chim. Miner.*, 1980, **17**, 458–465.

95 Z. L. Jian, L. Zhao, H. L. Pan, Y. S. Hu, H. Li, W. Chen and L. Q. Chen, *Electrochem. Commun.*, 2012, **14**, 86–89.

96 Y. Uebou, T. Kiyabu, S. okada and J.-I. Yamaki, *The Reports of Institute of Advanced Materials Study*, 2002, **16**, 1–5.

97 L. S. Plashnitsa, E. Kobayashi, Y. Noguchi, S. Okada and J. Yamaki, *J. Electrochem. Soc.*, 2010, **157**, A536–A543.

98 Z. L. Jian, W. Z. Han, X. Lu, H. X. Yang, Y.-S. Hu, J. Zhou, Z. B. Zhou, J. Q. Li, W. Chen, D. F. Chen and L. Q. Chen, *Adv. Energy Mater.*, 2013, **3**, 156–160.

99 D. Wang, X. Wu, Z. Wang and L. Chen, *J. Power Sources*, 2005, **140**, 125–128.

100 J. Kang, S. Baek, V. Mathew, J. Gim, J. Song, H. Park, E. Chae, A. K. Rai and J. Kim, *J. Mater. Chem.*, 2012, **22**, 20857–20860.

101 K. Saravanan, C. W. Mason, A. Rudola, K. H. Wong and P. Balaya, *Adv. Energy Mater.*, 2013, **3**, 444–450.

102 S. Y. Lim, H. Kim, R. A. Shakoor, Y. Jung and J. W. Choi, *J. Electrochem. Soc.*, 2012, **159**, A1393–A1397.

103 N. Anantharamulu, K. K. Rao, G. Rambabu, B. V. Kumar, V. Radha and M. Vithal, *J. Mater. Sci.*, 2011, **46**, 2821–2837.

104 M. Hidouri, B. Lajmi, A. Wattiaux, U. Fournes, J. Darriet and M. B. Amara, *J. Solid State Chem.*, 2004, **177**, 55–60.

105 S. Khorari, A. Rulmont and P. Tarte, *J. Solid State Chem.*, 1997, **131**, 290–297.

106 A. Feltz, S. Barth, M. Andratschke and C. Jager, *J. Less Common Met.*, 1988, **137**, 43–54.

107 M. Chakir, A. El Jazouli and D. de Waal, *J. Solid State Chem.*, 2006, **179**, 1883–1891.

108 C. Delmas, F. Cherkaoui, A. Nadiri and P. Hagenmuller, *Mater. Res. Bull.*, 1987, **22**, 631–639.

109 S. Il Park, I. Gocheva, S. Okada and J. Yamaki, *J. Electrochem. Soc.*, 2011, **158**, A1067–A1070.

110 P. Senguttuvan, G. Rousse, M. E. Arroyo y de Dompablo, H. Vezin, J. M. Tarascon and M. R. Palacín, *J. Am. Chem. Soc.*, 2013, **135**, 3897–3903.

111 P. B. Moore, *Am. Mineral.*, 1971, **56**, 1955–1975.

112 K. Trad, D. Carlier, L. Croguennec, A. Wattiaux, M. Ben Amara and C. Delmas, *Chem. Mater.*, 2010, **22**, 5554–5562.

113 T. J. Richardson, *J. Power Sources*, 2003, **119**, 262–265.

114 K. Trad, D. Carlier, L. Croguennec, A. Wattiaux, M. Ben Amara and C. Delmas, *Inorg. Chem.*, 2010, **49**, 10378–10389.

115 J. Barker, R. K. B. Gover, P. Burns and A. Bryan, *Electrochem. Solid-State Lett.*, 2005, **8**, A285–A287.

116 Y. Kawabe, N. Yabuuchi, M. Kajiyama, N. Fukuhara, T. Inamasu, R. Okuyama, I. Nakai and S. Komaba, *Electrochemistry*, 2012, **80**, 80–84.

117 R. K. B. Gover, A. Bryan, P. Burns and J. Barker, *Solid State Ionics*, 2006, **177**, 1495–1500.

118 R. A. Shakoor, D. H. Seo, H. Kim, Y. U. Park, J. Kim, S. W. Kim, H. Gwon, S. Lee and K. Kang, *J. Mater. Chem.*, 2012, **22**, 20535–20541.

119 J. Barker, M. Y. Saidi and J. L. Swoyer, *Electrochem. Solid-State Lett.*, 2003, **6**, A1–A4.

120 J. Barker, M. Y. Saidi and J. L. Swoyer, *J. Electrochem. Soc.*, 2004, **151**, A1670–A1677.

121 H. T. Zhuo, X. Y. Wang, A. P. Tang, Z. M. Liu, S. Gamboa and P. J. Sebastian, *J. Power Sources*, 2006, **160**, 698–703.

122 P. Serras, V. Palomares, A. Goni, I. G. de Muro, P. Kubiak, L. Lezama and T. Rojo, *J. Mater. Chem.*, 2012, **22**, 22301–22308.

123 P. Serras, V. Palomares, A. Goñi, P. Kubiak and T. Rojo, *J. Power Sources*, 2013, **241**, 56–60.

124 B. L. Ellis, W. R. M. Makahnouk, Y. Makimura, K. Toghill and L. F. Nazar, *Nat. Mater.*, 2007, **6**, 749–753.

125 A. Langrock, Y. H. Xu, Y. H. Liu, S. Ehrman, A. Manivannan and C. S. Wang, *J. Power Sources*, 2013, **223**, 62–67.

126 S. W. Kim, D. H. Seo, H. Kim, K. Y. Park and K. Kang, *Phys. Chem. Chem. Phys.*, 2012, **14**, 3299–3303.
127 M. Nishijima, I. D. Gocheva, S. Okada, T. Doi, J. Yamaki and T. Nishida, *J. Power Sources*, 2009, **190**, 558–562.
128 Y. Yamada, T. Doi, I. Tanaka, S. Okada and J. Yamaki, *J. Power Sources*, 2011, **196**, 4837–4841.
129 C. D. Wessells, R. A. Huggins and Y. Cui, *Nat. Commun.*, 2011, **2**, 550.
130 C. D. Wessells, S. V. Peddada, R. A. Huggins and Y. Cui, *Nano Lett.*, 2011, **11**, 5421–5425.
131 M. Pasta, C. D. Wessells, R. A. Huggins and Y. Cui, *Nat. Commun.*, 2012, **3**, 1149.
132 Y. H. Lu, L. Wang, J. G. Cheng and J. B. Goodenough, *Chem. Commun.*, 2012, **48**, 6544–6546.
133 L. Wang, Y. H. Lu, J. Liu, M. W. Xu, J. G. Cheng, D. W. Zhang and J. B. Goodenough, *Angew. Chem., Int. Ed.*, 2013, **52**, 1964–1967.
134 J. F. Qian, M. Zhou, Y. L. Cao, X. P. Ai and H. X. Yang, *Adv. Energy Mater.*, 2012, **2**, 410–414.
135 P. Novak, K. Muller, K. S. V. Santhanam and O. Haas, *Chem. Rev.*, 1997, **97**, 207–281.
136 H. Chen, M. Armand, G. Demailly, F. Dolhem, P. Poizot and J. M. Tarascon, *ChemSusChem*, 2008, **1**, 348–355.
137 B. Genorio, K. Pirnat, R. Cerc-Korosec, R. Dominko and M. Gaberscek, *Angew. Chem., Int. Ed.*, 2010, **49**, 7222–7224.
138 B. V. Ratnakumar, S. Distefano, R. M. Williams, G. Nagasubramanian and C. P. Bankston, *J. Appl. Electrochem.*, 1990, **20**, 357–364.
139 R. Zhao, L. Zhu, Y. Cao, X. Ai and H. X. Yang, *Electrochem. Commun.*, 2012, **21**, 36–38.
140 M. Zhou, L. Zhu, Y. Cao, R. Zhao, J. Qian, X. Ai and H. Yang, *RSC Adv.*, 2012, **2**, 5495–5498.
141 K. Sakaushi, E. Hosono, G. Nickerl, T. Gemming, H. Zhou, S. Kaskel and J. Eckert, *Nat. Commun.*, 2013, **4**, 1485.
142 K. Nobuhara, H. Nakayama, S. Nakanishi and H. Iba, *Meet. Abstr.*, 2012, **MA2012–02**, 1854.
143 D. P. Divincenzo and E. J. Mele, *Phys. Rev. B*, 1985, **32**, 2538–2553.
144 M. M. Doeff, Y. P. Ma, S. J. Visco and L. C. Dejonghe, *J. Electrochem. Soc.*, 1993, **140**, L169–L170.
145 D. A. Stevens and J. R. Dahn, *J. Electrochem. Soc.*, 2000, **147**, 1271–1273.
146 K. Gotoh, T. Ishikawa, S. Shimadzu, N. Yabuuchi, S. Komaba, K. Takeda, A. Goto, K. Deguchi, S. Ohki, K. Hashi, T. Shimizu and H. Ishida, *J. Power Sources*, 2013, **225**, 137–140.
147 P. Thomas and D. Billaud, *Electrochim. Acta*, 2002, **47**, 3303–3307.
148 S. Wenzel, T. Hara, J. Janek and P. Adelhelm, *Energy Environ. Sci.*, 2011, **4**, 3342–3345.
149 K. Tang, L. J. Fu, R. J. White, L. H. Yu, M. M. Titirici, M. Antonietti and J. Maier, *Adv. Energy Mater.*, 2012, **2**, 873–877.
150 Y. L. Cao, L. F. Xiao, M. L. Sushko, W. Wang, B. Schwenzer, J. Xiao, Z. M. Nie, L. V. Saraf, Z. G. Yang and J. Liu, *Nano Lett.*, 2012, **12**, 3783–3787.
151 H.-G. Wang, Z. Wu, F.-I. Meng, D.-l. Ma, X.-l. Huang, L.-M. Wang and X.-B. Zhang, *ChemSusChem*, 2013, **6**, 56–60.
152 S. Komaba, W. Murata, T. Ishikawa, N. Yabuuchi, T. Ozeki, T. Nakayama, A. Ogata, K. Gotoh and K. Fujiwara, *Adv. Funct. Mater.*, 2011, **21**, 3859–3867.
153 R. Alcantara, M. Jaraba, P. Lavela and J. L. Tirado, *Chem. Mater.*, 2002, **14**, 2847–2848.
154 Q. Sun, Q. Q. Ren, H. Li and Z. W. Fu, *Electrochem. Commun.*, 2011, **13**, 1462–1464.
155 S. Komaba, T. Mikumo and A. Ogata, *Electrochem. Commun.*, 2008, **10**, 1276–1279.
156 B. Koo, S. Chattopadhyay, T. Shibata, V. B. Prakapenka, C. S. Johnson, T. Rajh and E. V. Sheychenko, *Chem. Mater.*, 2013, **25**, 245–252.
157 K. M. Colbow, J. R. Dahn and R. R. Haering, *J. Power Sources*, 1989, **26**, 397–402.
158 E. Ferg, R. J. Gummow, A. Dekock and M. M. Thackeray, *J. Electrochem. Soc.*, 1994, **141**, L147–L150.
159 P. Senguttuvan, G. Rousse, V. Seznec, J. M. Tarascon and M. R. Palacin, *Chem. Mater.*, 2011, **23**, 4109–4111.
160 W. Wang, C. J. Yu, Y. J. Liu, J. G. Hou, H. M. Zhu and S. Q. Jiao, *RSC Adv.*, 2013, **3**, 1041–1044.
161 A. Rudola, K. Saravanan, C. W. Mason and P. Balaya, *J. Mater. Chem. A*, 2013, **1**, 2653–2662.
162 W. Wang, C. Yu, Z. Lin, J. Hou, H. Zhu and S. Jiao, *Nanoscale*, 2013, **5**, 594–599.
163 H. L. Pan, X. Lu, X. Q. Yu, Y.-S. Hu, H. Li, X.-Q. Yang and L. Q. Chen, *Adv. Energy Mater.*, 2013, DOI: 10.1002/aenm.201300139.
164 H. Xiong, M. D. Slater, M. Balasubramanian, C. S. Johnson and T. Rajh, *J. Phys. Chem. Lett.*, 2011, **2**, 2560–2565.
165 L. Zhao, H. L. Pan, Y. S. Hu, H. Li and L. Q. Chen, *Chin. Phys. B*, 2012, **21**, 028201.
166 Y. Sun, L. Zhao, H. L. Pan, X. Lu, L. Gu, Y.-S. Hu, H. Li, M. Armand, Y. Ikuhara, L. Q. Chen and X. J. Huang, *Nat. Commun.*, 2013, **4**, 1870.
167 X. Lu, L. Zhao, X. He, R. Xiao, L. Gu, Y.-S. Hu, H. Li, Z. Wang, X. Duan, L. Chen, J. Maier and Y. Ikuhara, *Adv. Mater.*, 2012, **24**, 3233–3238.
168 J. S. Kim, H. J. Ahn, H. S. Ryu, D. J. Kim, G. B. Cho, K. W. Kim, T. H. Nam and J. H. Ahn, *J. Power Sources*, 2008, **178**, 852–856.
169 T. B. Kim, W. H. Jung, H. S. Ryu, K. W. Kim, J. H. Ahn, K. K. Cho, G. B. Cho, T. H. Nam, I. S. Ahn and H. J. Ahn, *J. Alloys Compd.*, 2008, **449**, 304–307.
170 C. K. Chan, H. L. Peng, G. Liu, K. McIlwrath, X. F. Zhang, R. A. Huggins and Y. Cui, *Nat. Nanotechnol.*, 2008, **3**, 31–35.
171 G. Derrien, J. Hassoun, S. Panero and B. Scrosati, *Adv. Mater.*, 2007, **19**, 2336–2340.
172 S. Komaba, Y. Matsuura, T. Ishikawa, N. Yabuuchi, W. Murata and S. Kuze, *Electrochem. Commun.*, 2012, **21**, 65–68.
173 V. L. Chevrier and G. Ceder, *J. Electrochem. Soc.*, 2011, **158**, A1011–A1014.
174 J. F. Qian, Y. Chen, L. Wu, Y. L. Cao, X. P. Ai and H. X. Yang, *Chem. Commun.*, 2012, **48**, 7070–7072.

175 L. F. Xiao, Y. L. Cao, J. Xiao, W. Wang, L. Kovarik, Z. M. Nie and J. Liu, *Chem. Commun.*, 2012, **48**, 3321–3323.
176 Y. H. Xu, Y. J. Zhu, Y. H. Liu and C. S. Wang, *Adv. Energy Mater.*, 2013, **3**, 128–133.
177 J. Qian, X. Wu, Y. Cao, X. Ai and H. Yang, *Angew. Chem., Int. Ed.*, 2013, **52**, 4633–4636.
178 Y. Kim, Y. Park, A. Choi, N.-S. Choi, S. M. Oh and K. Lee, *Adv. Mater.*, 2013, **25**, 3045–3049.
179 J. W. Wang, X. H. Liu, S. X. Mao and J. Y. Huang, *Nano Lett.*, 2012, **12**, 5897–5902.
180 H. Li, Z. Wang, L. Chen and X. Huang, *Adv. Mater.*, 2009, **21**, 4593–4607.
181 M. Armand, S. Grugeon, H. Vezin, S. Laruelle, P. Ribiere, P. Poizot and J. M. Tarascon, *Nat. Mater.*, 2009, **8**, 120–125.
182 L. Zhao, J. M. Zhao, Y. S. Hu, H. Li, Z. B. Zhou, M. Armand and L. Q. Chen, *Adv. Energy Mater.*, 2012, **2**, 962–965.
183 Y. Park, D. S. Shin, S. H. Woo, N. S. Choi, K. H. Shin, S. M. Oh, K. T. Lee and S. Y. Hong, *Adv. Mater.*, 2012, **24**, 3562–3567.
184 A. Abouimrane, W. Weng, H. Eltayeb, Y. J. Cui, J. Niklas, O. Poluektov and K. Amine, *Energy Environ. Sci.*, 2012, **5**, 9632–9638.
185 K. Chihara, N. Chujo, A. Kitajou and S. Okada, 2013, DOI: 10.1016/j.electacta.2013.1004.1100.
186 Y. S. Hu, W. H. Kong, L. Hong, X. J. Huang and L. Q. Chen, *Electrochem. Commun.*, 2004, **6**, 126–131.
187 Y. S. Hu, W. H. Kong, Z. X. Wang, H. Li, X. J. Huang and L. Q. Chen, *Electrochem. Solid-State Lett.*, 2004, **7**, A442–A446.
188 Y. S. Hu, W. H. Kong, Z. X. Wang, X. J. Huang and L. Q. Chen, *Solid State Ionics*, 2005, **176**, 53–56.
189 L. Suo, Y.-S. Hu, H. Li, M. Armand and L. Q. Chen, *Nat. Commun.*, 2013, **4**, 1481.
190 A. Ponrouch, E. Marchante, M. Courty, J. M. Tarascon and M. R. Palacin, *Energy Environ. Sci.*, 2012, **5**, 8572–8583.
191 C. Ding, T. Nohira, K. Kuroda, R. Hagiwara, A. Fukunaga, S. Sakai, K. Nitta and S. Inazawa, *J. Power Sources*, 2013, **238**, 296–300.
192 S. Komaba, T. Ishikawa, N. Yabuuchi, W. Murata, A. Ito and Y. Ohsawa, *ACS Appl. Mater. Interfaces*, 2011, **3**, 4165–4168.
193 J. T. Kummer and N. Weber, *SAE Trans.*, 1968, **76**, 1003–1005.
194 O. Bohnke, S. Ronchetti and D. Mazza, *Solid State Ionics*, 1999, **122**, 127–136.
195 A. Hayashi, K. Noi, A. Sakuda and M. Tatsumisago, *Nat. Commun.*, 2012, **3**, 856.
196 X. Wu, Y. Cao, X. Ai, J. Qian and H. Yang, *Electrochem. Commun.*, 2013, **31**, 145–148.
197 S. P. Ong, V. L. Chevrier, G. Hautier, A. Jain, C. Moore, S. Kim, X. H. Ma and G. Ceder, *Energy Environ. Sci.*, 2011, **4**, 3680–3688.